Luttinger-liquid theory of purple bronze Li$_{0.9}$Mo$_6$O$_{17}$ in the charge regime

P. Chudzinski, T. Jarlborg, and T. Giamarchi

DPMC, University of Geneva, 24 Quai Ernest-Ansermet, CH-1211 Geneva 4, Switzerland

Molybdenum purple bronze Li$_{0.9}$Mo$_6$O$_{17}$ is an exceptional material known to exhibit one-dimensional (1D) properties for energies down to a few meV. This fact seems to be well established both in experiments and in band structure theory. We use the unusual, very 1D band dispersion obtained in *ab initio* DFT-LMTO band calculations as our starting point to study the physics emerging below 300 meV. A dispersion perpendicular to the main dispersive direction is obtained and investigated in detail. Based on this, we derive an effective low-energy theory within the Tomonaga-Luttinger liquid (TLL) framework. We estimate the strength of the possible interactions and from this deduce the values of the TLL parameters for charge modes. Finally, we investigate possible instabilities of TLL by deriving renormalization group equations which allow us to predict the size of potential gaps in the spectrum. While $2k_F$ instabilities strongly suppress each other, the $4k_F$ instabilities cooperate, which paves the way for a possible charge-density wave at the lowest energies. The aim of this work is to understand the experimental findings, in particular the ones which are certainly lying within the 1D regime. We discuss the validity of our 1D approach and further perspectives for the lower-energy phases.

I. INTRODUCTION

The molybdenum purple bronze, Li$_{0.9}$Mo$_6$O$_{17}$, is a subject of intensive experimental studies already for more than two decades,[1] but its unusual properties remain unclear. Several very different experimental probes have been used: angle-resolved photoemission spectroscopy (ARPES),[2] scanning tunneling microscopy (STM),[3] dc,[4] and magnetoresistivity,[5] thermal conductivity,[6] optical conductivity,[7] Nernst signal,[8] muons spectroscopy,[9] x rays,[10] thermal expansion,[11] neutron scattering.[12] Although the main effort of those investigations was focused on the nature of a mysterious phase transition at around 25 K, interesting knowledge about higher energy phase was also gathered. Certain properties of the one-dimensional (1D) metal, the Tomonaga-Luttinger liquid (TLL), have been invoked to explain the measured data[2,3,13,14] and nowadays the presence of the 1D physics is well established experimentally,[15,16] at least in some energy range.

On the theoretical side, band structure calculations have shown[17–19] a quasi-1D character of molybdenum purple bronze. A remarkably simple band structure emerges from rather complex crystal structure. At the Fermi surface there are only two bands, lying very close to each other, in the form of flat sheets dispersing well only along the *b* axis. This gives a hope that purple bronze can indeed be a rare realization of the 1D physics.

The key problem is that several possible mechanisms have been invoked to explain the observed properties, which made the subject quite unclear and controversial. In our opinion the reason for this situation is that each of previous attempts was focused only on one of many peculiar properties of Li$_{0.9}$Mo$_6$O$_{17}$ and most of them searched for an explanation in the low-energy regime (below 5 meV), where indeed the properties of Li$_{0.9}$Mo$_6$O$_{17}$ are the most spectacular. By now, not enough attention has been paid even to the parameters of the 1D state. It is only agreed that it emerges at energies as high as 250 meV. The values of these parameters are the first issue one must determine before pursuing research towards low-energy regimes. The unusual physics observed in Li$_{0.9}$Mo$_6$O$_{17}$ at the energy scales of order 10 meV is obviously a motivation for revising the question of the 1D physics. In order to establish a proper low-energy effective theory one has to begin at highest energies and move step by step towards the physics taking place around Fermi energy. The first step is to link the results of the DFT calculations with the well-defined field theory describing the experimental results at around 20 meV. It is this "high-energy" regime which must be well understood first. This is the main task of this paper.

The central result of this paper consists of the values of TLL parameters, which determine the physics taking place in the high-energy regime. As the 1D theory undoubtedly holds for these energy scales this allows for a meaningful comparison with experiments. We find a good agreement with measured values and discuss possible finite temperature deviations emerging from structural degrees of freedom.[17] We also assess the validity of our theory by inspecting the amplitudes and relevancy of several possible perturbations.

The plan of this work is as follows. In Sec. II we begin with a brief introduction of the band structure. In Sec. III A we propose a tight-binding model which is able to approximate bands around the Fermi energy E_F; however, in addition, it contains also the strong correlation terms beyond the LDA-DFT. In Sec. III B we give basic notions of 1D physics used in the rest of the paper. Section IV is dedicated to intrachain physics: We give values parameterizing strong correlations (Sec. IV A), estimate TLL parameters which this implies (Sec. IV B), and give energy scales for the spin sector (Sec. IV D). In Sec. V we introduce the interchain physics. Once again, first we estimate the strength of these interactions (Sec. V A) and then (Sec. V B) cast as many of them as possible into effective LL description, now within the ladder framework. Later in Sec. VI we study how the nonlinear interaction terms will affect the Luttinger liquid parameters and what instabilities they can potentially produce. Finally, in Sec. VII we discuss our results for LL parameters in a context of the experimental findings (Sec. VII A), as well as the validity of the 1D approach itself in Sec. VII B. We also
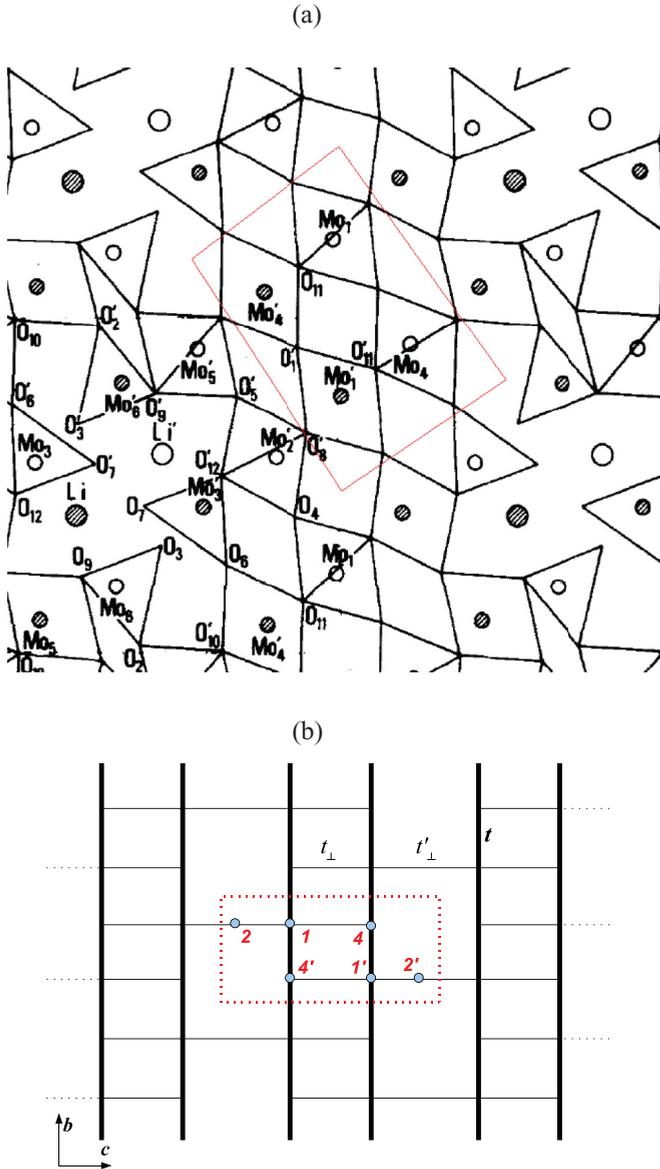
(a)

(b)

FIG. 1. (Color online) (a) The crystal structure of purple bronze, after Ref. 10. A cut perpendicular to highly conductive b axis is shown. The atoms which belongs to zig-zag chains are indicated. (b) A simplified structure of the low energy model. We show the top view on b-c plane. The t and $t_\perp$ hoppings as given in the first line of hamiltonian Eq. (2) are shown, sites 1 and 4 lie within the ladder, site 2 is outside it but $t_\perp$ hopping most likely goes through this site. Dotted (red) boxes indicate the unit cell within a conducting plane.

discuss in Sec. VIII the role of substitutional disorder in our model. The conclusions in Sec. IX close the paper.

II. BAND STRUCTURE

The lattice space group and atomic positions within the structure are known from experiment done by Onoda *et al.*[10] and recently have been confirmed by neutron diffraction experiment.[12] This rather complicated structure, which consists of well separated slabs parallel to the b-c plane, is presented in Fig. 1(a). Based on this crystallography knowledge the electronic structure of $Li_2Mo_{12}O_{34}$ can be calculated using

density functional theory (DFT), for example, in the local density approximation (LDA). Recent calculations[17] lead to results which are globally consistent with several previous computations.[18,19] Overall the band dispersions agree well with the measured results obtained by ARPES.[20] For example, it shows a flattening of the two dispersive bands at about 0.4–0.5 eV below E_F. Other bands are found at least 0.25 eV below E_F. The only visible discrepancies are the relative vertical shifts of the bands of order 0.1 eV. The computed ratio between the Fermi velocities along the b- and c-crystal axes, about 40, is compatible with the reported anisotropic 1D-like resistivity.[4,5,7,21] The velocity along $\vec{a}$ is even smaller. At low energies (around Fermi energy E_F) all calculations gave qualitatively similar results. There are only two bands which cross the Fermi energy and they are very close to each other. They have a strong dispersion in the Γ-Y direction (b axis) and barely any dispersion in the perpendicular directions.

The two bands originate from a pair of zig-zag chains built out of Mo atoms inside O octahedra. The low-energy (close to E_F) spectral function consists mostly of $4d$ (precisely t_{2g}) orbitals of Mo(1) and Mo(4) atoms, using the notation from Fig. 1(a). These two corners of zig-zag are symmetrically inequivalent; thus, dimerization is possible. However, their distinction arises more from out-of-chain than in-chain environment. The difference solely within a chain is hard to notice. It is also hard to distinguish the corresponding gap on the edge of Brillouin zone upon the analysis of the LDA band structure (in the following we assume that it is not larger than ∼0.1 eV).

The standard procedure (see Appendix A) is to fit the DFT band structure with an effective tight-binding model. Along the b axis (along the chains) the LDA calculations were done in the reduced Brillouin zone (because of the above-described presence of two inequivalent Mo sites). Then, in a tight-binding approximation, we expect that the band will be backfolded with a gap at the boundary of a reduced Brillouin zone which corresponds to the above-mentioned strength of dimerization (not larger than ∼0.1 eV). In $Li_2Mo_{12}O_{34}$, while it is rather easy to distinguish the lower half of the dispersing bands (however, there are some peculiarities at $k^c \approx \pi$), the upper half hybridizes strongly with other bands (originating mostly from oxygen orbitals). Their proper identification is then difficult. The band gap seems to be quite small; however, the presence of hybridization makes the estimate quite difficult. In the following we assume that it is $\leqslant 10\% t$, where $t \approx 0.8$ eV is hopping along the chain.

Along the c axis the dispersion relation is quite unusual (there is a node at zero momenta along this axis) and this peculiar feature appears within all independent DFT calculations.[17–19] Here we are also dealing with the reduced Brillouin zone, but the presence of the node means that the standard backfolding does not apply. One has to try possible combinations of cosines (see Appendix A), keeping in mind two facts: unequal distances for intra- and interladder hopping and large distance between ladders (pairs of chains). These imply that the next-nearest-neighbor hopping must be very small [only the light dashed lines on Fig. 1(a) give nonzero contribution].

We were able to deduce (see Appendix A for details) that the hopping in the perpendicular direction $t_\perp$ is ∼15 meV [certainly smaller than 30 meV (≈300 K)]. One should also

notice a large frustration, change of sign, when hopping to the next-nearest chain (interladder hopping) with the amplitude of this hopping ∼10 meV. This change of sign can be ascribed to a phase shift acquired when hopping between pairs of chains, between two Mo_1 atoms via Mo_2 octahedra [see Fig. 1(a)].

Along the a axis we have well separated slabs, with a void between them filled by Li atoms and Mo(6), Mo(3) tetrahedra. Electrons residing there (if any) stay on energies a few eVs away from E_F. This explains the very low band dispersion in this direction.

Significant deviations from LDA were seen in ARPES only below 0.2 eV, where the two bands seems to merge. This is also the energy scale revealed by optics:[7] It shows a formation of a first plasmon edge for electrons along b axis (Γ-Y direction) and a gap value in perpendicular direction. Thus, it seems reasonable to take it as a point where the 1D physics forms. This is the starting point (on the high-energy side) of the present study.

III. EFFECTIVE LOW-ENERGY HAMILTONIANS

A. Tight-binding fermionic Hamiltonian

The LDA-DFT results presented in Sec. II treat electron-electron interactions at the mean field level. It is assumed that a single electron moves in an average electrostatic potential. However, it is known that the higher-order terms in electron-electron interaction can bring very different physics, particularly in the case of reduced dimensionality. Thus, we need to introduce them to our model.

The LDA results show that a majority of carriers at the Fermi energy is localized on zig-zag chains formed by the Mo(1) and Mo(4) octahedra [see Fig. 1(a)]. We can safely assume that the low-energy physics is described by the dynamics of these electrons. Then the low-energy Hamiltonian formally writes

$$H = -t_1^b \sum_{i \in \text{even}_b, \sigma} c_{i,\sigma}^\dagger c_{i+\vec{b},\sigma} - t_2^b \sum_{i \in \text{odd}_b, \sigma} c_{i,\sigma}^\dagger c_{i+\vec{b},\sigma}$$
$$-t_1^c \sum_{i \in \text{even}_c, \sigma} c_{i,\sigma}^\dagger c_{i+\vec{c},\sigma} - t_2^c \sum_{i \in \text{odd}_c, \sigma} c_{i,\sigma}^\dagger c_{i+\vec{c},\sigma}$$
$$-t^a \sum_{i,\sigma} c_{i,\sigma}^\dagger c_{i+\vec{a},\sigma} + \text{H.c.}$$
$$+ \sum_{m,n,\sigma,\sigma'} V_{n\text{LDA}}(r_m - r_n) c_{m,\sigma}^\dagger c_{n,\sigma'}^\dagger c_{n,\sigma'} c_{m,\sigma}, \quad (1)$$

where the vectors $\vec{b} = [0,b,0]$, $\vec{c} = [0,0,c]$, and $\vec{a} = [a,0,0]$ define the $Li_{0.9}Mo_6O_{19}$ crystal lattice, summation runs over all ladder sites and depends on the parity of a given site index along directions $\vec{b}$ and $\vec{c}$. The $V_{n\text{LDA}}(r_m - r_n)$ are the electron-electron interactions not included in the (mean field) DFT calculation and the sum goes through positions of all carriers. The t^{a-c} are hopping parameters along each crystal axis, as estimated in the previous section. As discussed there $t^a \approx 0$ (down to 0.1 meV) so we can neglect it for the high-energy range we are interested in. The electrons are moving exclusively within one slab (and mostly along the zig-zag chains). In Eq. (1) we kept only nearest-neighbor hopping, since they are expected to be the dominant ones. The $t_{1,2}^i$ indicate a possibility of dimerization, namely different

TABLE I. The values of parameters (given in meV) of the tight-binding Hamiltonian given in Eq. (A1) which fits best the LDA result (Ref. 17), the dispersion along the c axis.

$t_{\perp 1}$	$t_{\perp 2}$	$t'_{\perp 1}$	$t'_{\perp 2}$
15	5	−10	<5

hoppings along ith axis for even and odd bonds. Because Mo(1) and Mo(4) are crystallographically different we included the possibility that we are dealing with a dimerized chain, half filled in the reduced Brillouin zone. We denote the two corresponding hoppings by t_1^b and t_2^b. As explained in the previous section we take $t_1^b \approx t_2^b$ (with 10% accuracy). The $t_{1,2}^c$ describe intra- and interladder hopping, respectively (see Appendix A). To simplify the notations we denote from now on t^b by t and t^c by $t_\perp$ to emphasize that they correspond to hopping along and perpendicular to the chain direction, respectively.

The resulting simplified tight-binding model is shown on Fig. 1(b). We simplify the interactions in a similar way by explicitly considering the intrachain and interchain parts of the interactions. The microscopic Hamiltonian we take is given by

$$H = -t \sum_{\langle i,j \rangle,\sigma} c_{i,\sigma}^\dagger c_{j,\sigma} - t_{1\perp} \sum_{\langle i,j_1 \rangle,\sigma} c_{i,\sigma}^\dagger c_{j_1,\sigma}$$
$$- t_{2\perp} \sum_{\langle i,j_2 \rangle,\sigma} c_{i,\sigma}^\dagger c_{j_2,\sigma} + U \sum_i n_{i\uparrow} n_{i\downarrow}$$
$$+ \sum_{m \neq n,\sigma,\sigma'} V_{\text{in}}(r_m - r_n) c_{m,\sigma}^\dagger c_{n,\sigma'}^\dagger c_{n,\sigma'} c_{m,\sigma}$$
$$+ \sum_{m \neq n,\sigma,\sigma'} V_{\text{out}}(r_m - r_n) c_{m,\sigma}^\dagger c_{n,\sigma'}^\dagger c_{n,\sigma'} c_{m,\sigma}, \quad (2)$$

where $t = 0.8$ eV (see Table I) is hopping between nearest-neighboring i, j (denoted $\langle i,j \rangle$) molybdenum atoms along zig-zag chains (b axis) and $t_{1,2\perp}$ are a hoppings in a perpendicular direction, within a slab (c axis), between nearest neighbors; 1 is intraladder while 2 is interladder. The values of $t_{1,2\perp}$ are estimated in Appendix A and summarized in Table I. As already mentioned $t_\perp < 20$ meV, so we can treat it as a perturbation on the top of the intrachain physics.

The strong correlations [last two lines in Eq. (2)] are usually parameterized by several quantities, which enter into the effective Hamiltonian: U is the local on-site interaction between charge densities of opposite spin $n_{i\uparrow} = c_{i\uparrow}^\dagger c_{i\uparrow}$ (Hubbard term), $V_{\text{in}}(r)$ is the interaction of two carriers placed inside the same chain at a distance $r \neq 0$, and $V_{\text{out}}(r)$ is the interaction of two carriers placed in two different chains in a distance r [both $V_{\text{in}}(r)$ and $V_{\text{out}}(r)$ are defined assuming an environment for which the LDA screening is included]. We discuss their strength in Sec. IV A.

B. Bosonic field theory of a 1D system

In the following sections, it is shown that the interchain couplings (both hopping and interactions) are reasonably weak compared to the intrachain ones. We can thus anticipate the need to describe a strongly interacting 1D system. In such a case, a very convenient formalism to incorporate the strong

intra-chain interactions from the start is provided by the Luttinger liquid formalism.[22] This formalism makes it possible to describe non-Fermi liquid state, Tomonaga Luttinger liquid (TLL), that occurs in 1D as a result of the interactions.

The low-energy dynamics of such a state is captured by collective, bosonic modes representing charge and spin density fluctuations. These fluctuations are connected to the two fields $\phi_\nu(x)$, where $\nu = \rho$ for charge fluctuations and $\nu = \sigma$ for spin fluctuations (linked with the fluctuations of charge and spin density). These fields have two canonically conjugate fields $\theta_\nu(x)$ linked with the respective currents fluctuations. In terms of these collective variables the Hamiltonian reads[22]

$$H_0 = \sum_\nu \int \frac{dx}{2\pi} \left[(u_\nu K_\nu)(\pi \Pi_\nu)^2 + \left(\frac{u_\nu}{K_\nu} \right)(\partial_x \phi_\nu)^2 \right], \quad (3)$$

where $\Pi_\nu(x) = \frac{1}{\pi} \nabla \theta_\nu(x)$. All the intrachain interactions conserving the momentum are now only fixing the precise values of the parameters u_ν (the velocities of the corresponding charge or spin density modes) or K_ν (the Luttinger parameters which control the decay of the various correlation functions).

In particular, the local spectral function behaves as a power law $A(x = 0, \omega, T = 0) \sim \omega^\alpha$ with the following (interaction dependent) exponent:

$$\alpha = \frac{\left(K_\sigma + K_\sigma^{-1} + K_\rho + K_\rho^{-1} \right)}{4} - 1. \quad (4)$$

For spin-rotationally invariant case $K_\sigma = 1$; thus, interactions leading to the anomalous behavior affect only the charge sector.

We can thus take (3) as our starting point for the chain physics and study in the bosonized representation the effects of the various interchain coupling terms. This will ensure that at least the upper energy scales of the high-energy regime will be properly treated. The first step to determine the Luttinger parameters u_ν and K_ν is to estimate the strength of the various interactions, which we do in the following section (Sec. IV A). At energies lower than the Fermi energy E_F only two scattering channels are allowed: $q \approx 0$ and $q \approx 2k_F$ (plus eventually higher harmonics). All density-density interactions, with small q momentum exchange, can be incorporated into the Hamiltonian given by Eq. (3). They contribute to a highly nontrivial dependence of the TLL parameter K_ρ (see Sec. IV B).

The remaining interaction terms produce nonsolvable Hamiltonians of sine-Gordon type, which in general is a functional $F[]$ of cosine terms:

$$H_{\cos} = F[\cos(\sqrt{8} p \phi_\nu(x)), \cos(\sqrt{8} q \theta_\nu(x))], \quad (5)$$

where p, q indicate higher harmonics (scattering with larger momenta exchange). Due to these terms the total problem allows only for an approximate solution (at least in terms of continuous fields theory). The terms present in $H_{\cos}$ are derived from large momentum exchange interactions (of both intra- and interchain origin). This is why their presence is analyzed carefully in the further sections. They are usually treated using renormalization group (RG) transformations, which makes it possible to extract the terms that affect the most TLL physics. This usually enables one to find the existence of gaps in the spectrum of bosonic modes, sometimes even to predict the ground-state phase diagram. This kind of approach is applied in Sec. VI.

IV. INTRACHAIN PHYSICS

Let us first consider the physics taking place within a single chain. We want to obtain (in Sec. IV A) the values of the various intrachain interactions in Eq. (2) and from there (in Sec. IV B) the values of the Luttinger parameters for the Hamiltonian (3).

A. Strength of interactions

1. U: Local on-site interaction

A fully self-consistent calculation has been performed in Ref. 18 and a value $U = 6.4$ eV was found. This value seems at first sight surprisingly large (for $4d$ electrons), but a recent study using constrained RPA[23] makes it possible to understand this result. Although for bulk Mo $U \approx 3.8$ eV, it was convincingly shown that the suppression of the pure Coulomb value $U_0 \approx 14$ eV is mostly due to efficient screening in 3D of the d electrons. In our case (as discussed in detail below) the system is underscreened, which also leads to a significantly reduced plasmon frequency in comparison with that of pure Mo [from ~ 15 to 0.65 eV (Ref. 23)]. Thus, the value $U = 6.4$ eV is justified or probably even modest. Then, if we take previously estimated hopping t, we get $U/t \approx 8$.

Note that this makes the local repulsion by far the largest energy scale in the problem.

2. $V_{\rm in}$: Interaction inside a chain

In Hamiltonian Eq. (2) we defined intrachain nonlocal interaction $V_{\rm in}(r)$. In this section we discuss its strength both in real and in momentum space $V_{\rm in}(q)$. We are going to use shorthand notation $V_{\rm in} \equiv V_{\rm in}(r = b/2)$, as this is usually the single parameter which enters into so-called U-V model for a 1D chain. This parameter is much more difficult to estimate than $V_{\rm out}$ (see Sec. V A) as it involves the dynamics of the 1D metal. Rather than trying to estimate it directly from the interaction itself, we simply adjust the value to be put in Eqs. (2) and (3) in order to reproduce the experimental data on optical spectroscopy.

The idea[24,25] is based on two independent estimates of kinetic energy in the system. The first one is related (by the optical sum rule) to the plasmon (edge) frequency $I_p = \omega_p^2$ and gives us the total possible kinetic energy available for the given number of carriers. The same quantity can be computed as an integral I_σ of the optical conductivity $\sigma(\omega)$ (taken only over the highest conducting band). The point is that the second estimate gives us the real kinetic energy, renormalized by interactions.

Fortunately, the necessary data is available for $\text{Li}_{0.9}\text{Mo}_6\text{O}_{17}$. The value of of the plasmon frequency can be read out from Fig. 2 in Ref. 7 and gives $\omega_p = 0.65$ eV (ω_p extracted from the LDA[17] is even larger ≈ 1.1 eV). The sum rule integral I_σ was, in fact, already evaluated in Fig. 3 of Ref. 7. Determining the value of the first saturation from the plot has an unavoidable error attached to it. We take $I_\sigma \approx 0.35$ ($\pm 5\%$). This value is reasonable because at higher energies one expects that the other bands start to intervene. The rest of the procedure is straightforward; the ratio of bare and interaction-suppressed
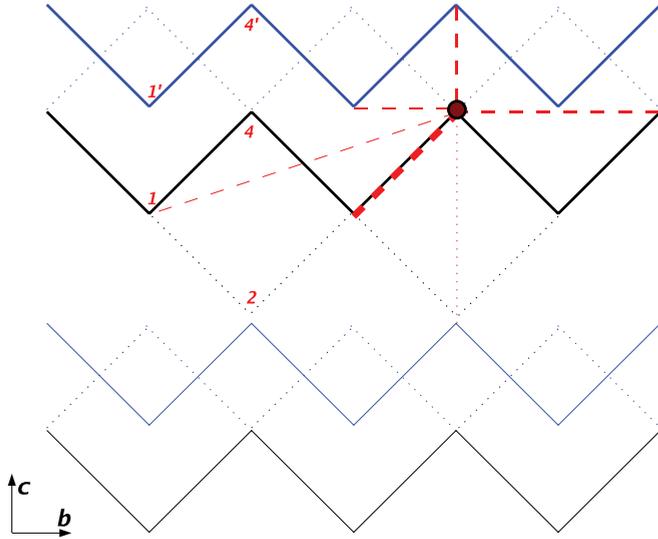
FIG. 2. (Color online) A real-space image of strong interactions terms possible in purple bronze; the top view of a conducting slab is given. Interactions between an electron located on a dot site and charges on different sites are indicated as red dashed lines of different thicknesses. Both V_{in} (dashed lines within a black chain) and V_{out} (dashed lines between the black and blue chains) are shown. The numbering of sites is like on Fig. 1.

kinetic energy I_σ/I_p equals to ≈ 0.83. Then the results of Ref. 25, together with the previously estimated value of U makes it possible to predict $V_{in}/t = 1.2$, which means $V_{in} = 0.95$ eV ($\pm > 5\%$).

In addition to the interactions discussed up to now (which fit within the U-V model for a single chain) there can also exist interactions between more distant neighbors (see Fig. 2). These interactions are nonzero because of the underscreening, a characteristic property of the 1D systems. When the separation is larger than that between nearest neighbor we can approximate the interaction by a continuum limit $V_{in}(r > b) = V_{Coul}(r)/\epsilon(r)$, where $b = 5.523$ Å is a lattice constant along the b axis[10] and $\epsilon(r)$ is a real-space dielectric constant. In 2D and 3D systems the electrostatic potential is usually well screened; thus, the Thomas-Fermi approximation, already used in the DFT calculation, is sufficient. In our problem this means that for the very long length scales $r \gg a$ the potential is well screened, $V(r \gg a) = 0$ (where $a = 12.762$ Å is the largest lattice constant, along the a axis, perpendicular to the slabs planes), because then the network of the zig-zag chains can be thought as a homogenous 3D bulk. For shorter distances between the interacting electrons $r \approx a$ and then the distance between the neighboring chains does matter. The relation $a = 2.1b$ implies that there are a few nonzero interaction terms $V_{in}(r)$ for $a \geqslant r > b$.

The screened potential inside 1D wire behaves approximately like $\ln(1/r)$,[22] and the same functional relation holds for the screening induced by the presence of other wires.[26] In total we approximate that $V_{in}(q = 0)$ will get renormalized by a factor $(1 + \ln(a/b)) \approx 1.6$. This gives a reasonable estimate for $V_{in}(q = 0)$; however, one has to be aware that for the value of charge mode TLL parameter the whole q structure has its importance.

TABLE II. The real-space values of strong coupling parameters (given in eV).

U	V_{in} $(r = b/2)$	V_{in} $(r = b)$	V_{in} $(r = 2b)$	V_{out} $(r = c)$	V_{out2} $(r = 2c)$
6.4	0.95($\pm > 5\%$)	0.5	0.2	0.55	0.2

The values of real and momentum space interactions are summarized in Tables II and III.

B. Values of TLL parameter in the charge sector

Clearly the density-density interactions caused by U and V are not small perturbations compared to the kinetic energy. In fact, they are the largest energy scale in the problem, larger than hopping along the chains. Thus, they strongly affect the charge sector; they are strong enough to give rise to well-pronounced non-Fermi liquid properties. We thus need to estimate the TLL parameters entering (3). As we prove in later sections, the following hierarchy of energies holds $U \gg V_{in} > t > V_{out} > J_{eff}$ (where J_{eff} is an effective superexchange which determines energy scales for spin sector).

We thus start by solving the TLL problem for a single chain and consider later the interchain couplings.

Even when $U \gg V_{in} > t$ we stay[27] in a gapless phase within the TLL universality class, but computing the values of the Luttinger liquid parameters K_ρ beyond the weak coupling limit is usually a very difficult problem,[22] since one cannot compute them perturbatively.

In the present case we have to deal with a quarter-filled system with a very small doping (δ around 2%), and a small dimerization (as we mentioned in Sec. III A it $t_1 - t_2$ cannot be larger than 10%t, we take moderately 5%t in any future calculations) and several nonzero interaction terms $V_{in}(r \geqslant b/2)$. As a first approximation we decided to analyze the physics of these zig-zag chains by looking at a quarter-filled extended Hubbard chain with a local interaction U and a nearest neighbor $V = V_{in}$.

If U is the largest energy scale in the problem, then the charge sector can be mapped onto a spinless chain of fermions (or an XXZ spin chain) for which the exact TLL parameters are known.[22,28] For a certain value V_{in} we have

$$K_\rho^{XXZ} = \frac{\pi}{4 \arccos\left[-\frac{V_{in}}{V_{in}^c(U)} \right]}, \quad (6)$$

where $V_{in}^c(U)$ is the critical value of intrachain nearest neighbor interaction for a given value U. When $U \to \infty$ the mapping is exact and the critical value is known $V_{in}^c(\infty) = 2t$. In this limit, when we substitute our V_{in} in Eq. (6) then we get $K_\rho^{XXZ} = 0.3$, which sets the lower limit for the TLL parameter in our problem. This is a rough estimate, but suggests that for further

TABLE III. The reciprocal space values of strong coupling parameters (given in eV).

V_{in} $(q = 0)$	V_{in} $(q = 2k_F)$	V_{out} $(q = 0)$	V_{out} $(q = 2k_F)$	V_{out} $(q = 4k_F)$
1.6	See Sec. VI B	0.55	< 0.05	0.05

analysis we should use approaches which are valid for the gapless phase.

A more precise estimate can be obtained from a numerical study of the extended Hubbard model and an estimation of the TLL parameters in the usual way via thermodynamic quantities.[28–30] From the relevant plots one reads out that our model is located somewhere in the range $K_\rho \in (0.3, 0.37)$. One can try to give an even better estimate using Eq. (6) even when U is not infinite (but still with U much larger that any other energy scale in the problem). It is commonly believed that the value $V_{in}^c(U)$ extracted from the numerics can give quite good approximation when substituted into Eq. (6). Estimates of critical $V_{in}^c(U)$ are usually done with higher precision than for arbitrary U, V. In our case $U = 8t$ implies $V_{in}^c(U) = 2.6t$[28,31] and $V_{in}^c(U) = 2.75t$ from older work by Mila and Zotos.[29] This gives $K_\rho = 0.330$ (with $V/V_c = 0.72$) or $K_\rho = 0.340$. We have also followed the critical scaling analysis proposed in Ref. 31 and found a similar value $K_\rho = 0.328$.

The exact solutions, for example, Bethe ansatz, are available for a few special cases. If we include a (quite weak) dimerization and (very small) doping, then the problem is located far away from any integrable model. However, the influence of both these perturbations are known. The dimerization is able to lower a bit value of K_ρ, this effect can be present in particular in our case when we are not far from V_{in}^c (Ref. 30). The doping has the opposite effect; however, when one is not very close to critical point $K_\rho^c = 1/4$ and close to commensurate case then the effect is negligible.

To conclude, the knowledge about the U, V_{in} we have collected above allowed us to give a several estimates based on complementary numerical calculations of U-V models. All these estimates gives $K_\rho \in (0.3; 0.36)$ (we allowed for 10% error in the U, V_{in} due to uncertainty of parameters). This is also in agreement with a very recent study for a system with finite range interaction:[32] $K_\rho \approx 1/3$ when we take a similar value of the on-site term and account for the presence of $V_{in}(r)$ interactions up to four to five Mo sites. However, in this last paper[32] interactions with an exponential character were studied, which means that they decay much faster than those in our problem.

Note that this K_ρ value is reasonably close to the one $K_\rho^* = 1/4$ that would lead to a quarter-filled Mott insulator in the presence of an infinitesimal V_{in}. The system will be thus very susceptible to the precise value of V_{in}. Given the accuracy of our estimation we take $K_\rho = 1/3$ for further calculations. This value corresponds to the case for which the $4k_F$ charge fluctuations decay with the same exponent as the $2k_F$ charge and spin density fluctuations.[22]

C. The remaining interaction terms

By now we have studied interactions in real space (which we believe can be useful for numerical studies), while cosine terms beyond the TLL general expression (3) are defined in the reciprocal space representation. These values of scattering for large momenta exchange will be used as an input for the discussion done in Sec. VI.

The Hubbard U interaction has a form of a δ function in real space; thus, in momentum space it contributes equally to small and large momenta exchange scattering (provided

they are the intrachain ones). The previous considerations also imply that, the Fourier transformed $V_{in}(q)$ is a weakly decaying function (slower than logarithm), so it affects the amplitude of scattering processes with large momenta exchange. As it was already expressed above, the intrachain interactions are much larger than t; thus, it is not straightforward to obtain the value of backscattering they cause. In fact, the $K_\rho = 1/3$ parameter given above, known from numerical studies of similar models, is a fixed point value K_ρ^*, which means that it contains a part of these contributions. Precisely, it is the part included in the simplified U-V model. The longer range and slower decaying interaction leads to smaller value of K_ρ^*. This suggests that the proper value of K_ρ^* in our problem, which contains long-range interactions, can be even smaller.

In our case the charge sector is renormalized by the possible umklapp terms g_3, so the last statement can be rephrased: A smaller final (fixed point) value of K_ρ^* can be linked to a larger value of initial, bare g_3^0. The precise estimation of the amplitude of g_3^0 is a very difficult task, the detailed discussion of the bare *large-q*, intrachain, term is done in Sec. VI.

In addition, the $\epsilon(r)$ when computed using RPA (beyond standard DFT) gives a well-known phenomena, the Friedel oscillations (in real space). The effect comes from the peculiar screening (singular susceptibility) at large momenta $q = 2k_F$. In our case, due to the value of k_F along chains, it gives an extra gain of energy for electrons located at every second site. This affects the large momentum exchange part of interaction $V_{in}(q \sim 4k_F)$. The value of this gain can be estimated using the fact that, for 3D metal, the additional oscillating part $V(r) \sim r^{-3}$. Thus, we give an estimation $V_{Frid} \leqslant V_{in}(r = b)/8 = 0.1$ eV. It is not as large as U or V, but can be significant if we compare it with $t_\perp$.

The U-V model that we have considered so far (in particular in Sec. IV B) is, of course, only an approximation of the intrachain physics and interactions. It should capture most of the effects at the energy scales we are considering; however, it may slightly underestimate the strength of interactions.

D. Spin mode

All the interactions considered up to now were connected with the charge sector. In 1D systems, because of the spin-charge separation, electron spin degree of freedom should be discussed separately. For a half-filled chain the knowledge about t and U makes it possible to estimate the spin-spin exchange (superexchange) constant $J = t\frac{4t}{U}$. This determines the energies at which the spin sector starts to play a role. The problem of purple bronze is more complex since the compound is quarter filled.

For such cases the formula for superexchange interaction can be still obtained from second-order perturbation theory.[30] It reads

$$J_{eff} = \frac{4t_2^2}{8t_1 + 2U + V_{in} - 2\sqrt{(U - V_{in})^2 + 16t_1^2}}, \quad (7)$$

where we have taken into a account the fact that due to dimerization there are two slightly different alternating hopping t_1 and t_2 along the chain. Taking $t_2 - t_1 \approx 0.05t$

and using the values of U and V_{in} obtained in Sec. IV A, we obtain

$$J_{\text{eff}} = 0.2 \text{ eV}. \tag{8}$$

It is indeed significantly smaller than t (and also the charge sector interactions U, V_{in}), which implies that charge dynamics will dominate the 0.2- to 0.02-eV energy range. However, it is a non-negligible value in the sense that even for energies as high as $\omega \sim 0.1$ eV (in the middle of the considered high-energy regime) the spin excitations are coherent and dispersion is linear; thus, a TLL description with spin and charge modes is applicable. The spin-incoherent TLL[33] is not an appropriate framework for our problem.

For a spin-rotational, SU(2) invariant model we have $K_\sigma(T = 0) = 1$. For the interacting case the spin velocity u_σ is smaller than $v_F \approx 2t$; in particular, $v_\sigma(U \to \infty) \to J$. This last value is comparable with the one observed in experiment.[13] The only candidate to break the SU(2) symmetry would be spin-orbit coupling D_{LS} on the heaviest atom, molybdenum. A series of experimental and LDA studies make it possible to set its value in bulk bcc Mo (Ref. 34) to $D_{LS} = 100$ meV. This value was obtained for the Δ point of a Brillouin zone in the Mo-bcc crystal. In our problem it should be smaller because the active electrons have mostly t_{2g} character (with a larger l quantum number). Thus, D_{LS} can be treated as a perturbation for J, contrary to U for t in a charge sector. This implies that K_σ deviates from the noninteracting value $K_\sigma = 1$ much less than K_ρ. To be precise, from weak coupling theory (applicable in this case) we know[22]

$$K_\sigma = \sqrt{\frac{1 + \frac{D_{LS}}{2\pi J}}{1 - \frac{D_{LS}}{2\pi J}}}, \tag{9}$$

from which we predict $K_\sigma = 1.1$, which can increase the Green's function exponent α only by 0.01. The spin sector thus cannot be responsible for the experimentally observed values of the α exponent [defined in Eq. (4)], which are of order ≈ 0.5. However, the influence of the spin-orbit coupling should be taken into account when one studies the physics taking place lower energy scales, which are beyond the scope of this paper.

V. PHYSICS BETWEEN THE CHAINS

After giving the description of a single-chain physics we move beyond this model and study the strength (and the role) of interactions between carriers moving in different chains.

A. V_{out}: The values of interactions between the chains

The density-density interactions can be estimated as a standard Coulomb interaction between charges in a 3D dielectric, as was done in Ref. 18. Those authors gave an estimate for a value of interaction from standard electrostatic Coulomb law (with the simplest static screening):

$$V_{out}(r = a) = \frac{1}{\kappa \epsilon_0 a}, \tag{10}$$

which, in fact, gives the value for two electrons in two different 2D slabs. We are more interested in interactions

inside the slab, which is obviously larger because (the smallest) interchain distance is then $c/2 = 0.4a$. A more fundamental problem is the value of the dielectric permittivity κ. In the previous work[18] the bulk $\bar\kappa \approx 10$ was used, which is typical for bulk semiconductors with similar value of a gap for oxygen states($\Delta_O \approx 2$ eV). Taking into account the very weak metallic character along the c axis the semiconductor approximation is correct. For further neighbors, with many oxygen atoms in between, one can take the bulk $\bar\kappa$ value. However, for the nearest chains, as there is only one row of oxygen atoms in the space between them, such a large κ value overestimates the screening.[35] It is then convenient to take a function $\kappa(r)$ such that $\kappa(c/2)$ is reduced by 30% in comparison with $\bar\kappa$. For larger r distances, at approximately $r \approx a$ it saturates to the bulk value $\bar\kappa$. With this set of values we estimate $V_{out} = 0.55$ eV. For $r \to \infty$ the metallic character along the b axis intervenes and $\kappa(r) \to \infty$. Thus, the large distance interaction is strongly suppressed. In such a case the above-estimated value for V_{out} can be taken as the density-density interaction [$V_{out}(q \sim 0)$] between the nearest chains. The above estimate was done between two nearest chains which form a pair (see Fig. 2). On the other side of each chain there is another neighbor which is placed two times further. According to Eq. (10) these interactions V_{out2} [we defined the inter-ladder term in analogy with, for example, t_{c2} in Eq. (A1)] are at least two times smaller. We then estimate [keeping $\kappa(r)$ in mind] $V_{out2} = 0.2$ eV.

The treatment of terms with *large momentum exchange* is more complex. There is a $q = 2k_F$ term which locks the interchain density wave, the so-called π-CDW (where CDW stands for charge-density wave), which is shown in Fig. 3(a). From the figure it is clear that the distances $r_\pi = \sqrt{(c/2)^2 + (2k_F)^{-2}}$ between charges in such configuration are rather large [around three times larger than the distance entering to previous calculation for $V_{out}(q = 0)$]; thus, the screening is quite efficient and $\kappa[r_\pi]$ is definitely not reduced, but probably even enhanced with respect to the bulk value. In fact, not only further chains, but also further slabs can intervene (because $r_\pi > a$).

There will be either a very efficient screening (like in a metal), or Coulomb potential approximation (but with enhanced κ) is still applicable. We assume, optimistically, the second case and use again Eq. (10). Two ways of proceeding are possible when one is interested in the staggered component of the interaction between two chains. In real space [direct application of (10)] one computes interactions with a linear set of dipoles. Due to increase of $\kappa(r)$ the interaction (with further dipoles) decays rapidly, which makes this straightforward approach quite tedious. In the reciprocal space approach one must take into account the fact that Fourier transform of $V_{out}(q)$ does decay in momentum space (it will be a $1/q$ decay in a 2D case corresponding to a separate slab). The second approach is simpler when one notices that the previously computed $V_{out} = 0.55$ eV corresponds to $q = 0 \pm (a/2)^{-1}$ (a distance between slabs sets the large distance cutoff). Then the $1/q$ scaling makes it possible to estimate that the $q = 2k_F$ term will be suppressed by an extra factor of four. Overall, we have

(i) a factor of 1.5–2 from the value $\kappa(r_\pi)$;
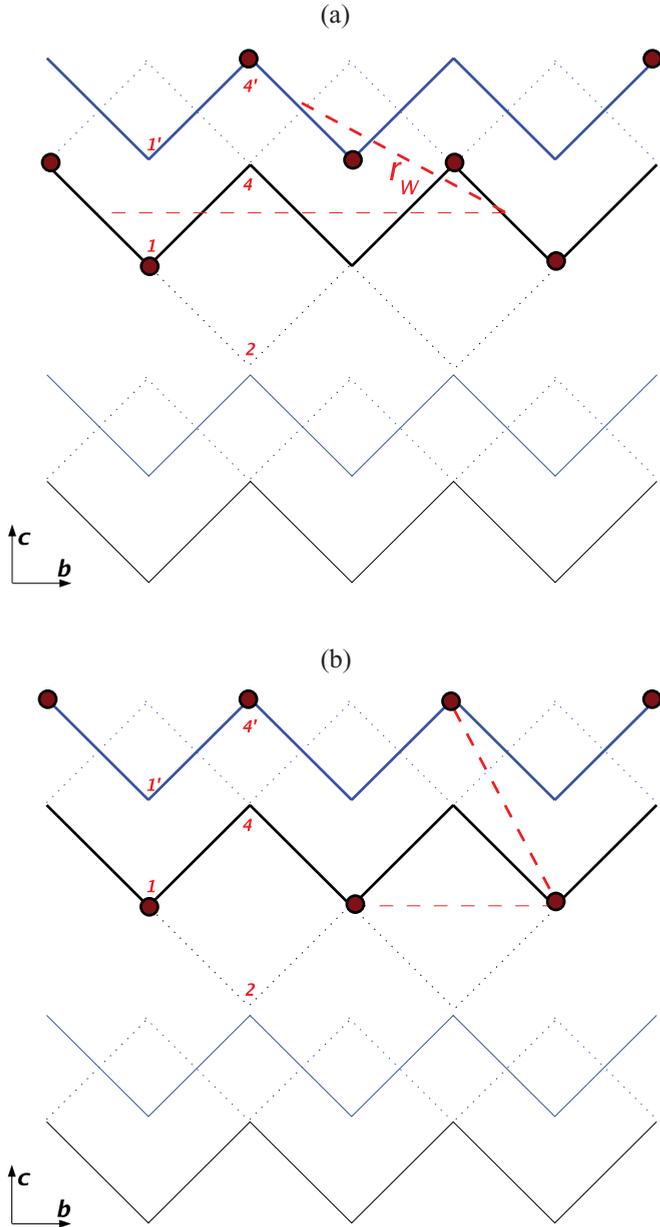(ii) a factor of 1.5–3 from the distance r_π;

FIG. 3. (Color online) A schematic side view of a ladder structure (which enters the low-energy description of purple bronze) with (a) the $2k_F$ π-DW instability shown (the light, dashed line correspond to the distance r_π) and (b) the $4k_F$ π-DW instability shown.

(iii) a factor of ≈ 4 because we compute the staggered (large q) component.

Taking all these factors into account, we estimate that the $2k_F$ component is reduced by at least one order of magnitude, which means $V_{\text{out}}(q = 2k_F) < 0.05$ eV.

There is also the $q = 4k_F$ term. Now the distance is smaller; thus, κ is unaffected. However, this term is strongly suppressed due to above-mentioned Coulomb character of $V_{\text{out}}(q)$. At short distances corresponding to $r = (4k_F)^{-1}$ the interaction may even have a 3D character (with no screening); thus, $V_{\text{out}} \sim q^2$. By a similar reasoning as given above, we get $V_{\text{out}}(q = 4k_F) \approx 0.05$ eV. The smallness of interchain large momenta terms (in comparison with density-density term) implies that the

local field corrections are small, so our mean field model of screening is self-consistent. The influence of the interchain exchange interactions (both $2k_F$ and $4k_F$) on 1D physics is discussed in Sec. VI.

To summarize the results for values of the strong coupling parameters found in the last two sections, we present all parameters in the Tables II and III.

B. Luttinger liquid framework

The density-density interaction between the two neighboring chains $V_{\text{out}}(q = 0)$ can be included on nonperturbative level. Because of the hierarchy of energies the presence of V_{out} should be included on the top of 1D chain K_ρ. The zig-zag chains are grouped in pairs as shown on Fig. 1(b). Inside each pair we have two short links with interaction V_{out} while in between them there is only one link with much smaller interaction V_{out2}. The ladder picture is then justified.

In the case of the ladderlike system (which means that there is either much stronger intraladder hopping $t_{1\perp} \gg t_{2\perp}$ or interaction) two more modes must be introduced. The problem can then be expressed in two different possible bases. One may work either in the chain basis with $\nu = \sigma 1, \sigma 2$ spin modes or in the total/transverse basis with symmetric and antisymmetric spin modes $\nu = \sigma S, \sigma A$ (and respectively the same for the charge sector). In general, the Green's function α exponent can be expressed as

$$\alpha = \frac{\sum_\nu^N \left(K_\nu + K_\nu^{-1}\right)}{2N} - 1, \quad (11)$$

where N is a number of modes. A significant $V_{\text{out}}(q = 0)$ gives a preference for symmetric and antisymmetric modes as it can be diagonalized in this basis.

Thus, within the ladder picture the two degenerate charge modes (in the two chains of the ladder) split into two holons with two different velocities. One of the holons (symmetric) describes the fluctuations of the total charge density, while the other one (antisymmetric) describes the relative fluctuations in two different zig-zag chains. The values of their TLL parameters are

$$K_{\rho S, A} = \frac{K_\rho}{\sqrt{1 \mp K_\rho V_{\text{out}}/(\pi^2 u_\rho)}}, \quad (12)$$

where in the above formula $V_{\text{out}} \equiv V_{\text{out}}(q = 0)$, K_ρ and u_ρ are TLL parameter and velocity of intrachain holon without interchain interactions included. The TLL parameter K_ρ has been discussed extensively in Sec. IV B and for our problem we can take $u_\rho \approx v_F$ (Ref. 37). Then the respective values, at the TLL fixed point ($\Lambda \to 0$), are $K_{\rho S} \approx 0.32$ and $K_{\rho A} \approx 0.36$. The relation $u_{\rho A}/u_{\rho S} = K_{\rho S}/K_{\rho A}$ implies that the velocities of two holons differs by around 10%.

For energies well below V_{out} the Hamiltonian of the charge sector is given as a sum of two bosonic modes plus a nonlinear part $H_{\cos}$ caused by large-q (exchange) interactions:

$$H_{\text{eff}} = \sum_\nu \int \frac{dx}{2\pi} \left[(u_\nu K_\nu)(\pi \Pi_\nu)^2 + \left(\frac{u_\nu}{K_\nu}\right) (\partial_x \phi_\nu)^2 \right] + H_{\cos}, \quad (13)$$

where, as explained in Sec. III B, now the summation goes over four modes $\nu = \rho S, \rho A, \sigma S, \sigma A$. If we neglect $H_{\cos}$ then the single-hole propagator (relevant for ARPES), the density Green's function with chirality ϑ,

$$G_\vartheta^<(x,t) = \langle \psi_{\vartheta,\sigma}^\dagger(x,t)\psi_{\vartheta,\sigma}(0,0)\rangle, \qquad (14)$$

is known[38] and can be written as a simple generalization of the standard TLL result, as a product of four gapless modes. For example, for the right-going hole,

$$G_R^<(x,t) = \prod_\nu g_{\zeta_\nu}(x,t), \qquad (15)$$

where

$$g_{\zeta_\nu} = [(x - v_\nu t)]^{\zeta_\nu}[(x + v_\nu t)]^{\zeta_\nu},$$

with the exponents $\zeta_\nu = (K_\nu + K_\nu^{-1})/8$. For a numerical values of these exponents in our model and their implications, see Sec. VII A.

In the case when $H_{\cos}$ is able to open a gap in a given mode, the respective term in the product in Eq. (15) should be substituted by a modified Bessel function of a second kind, which gives the expected exponential decay of correlation function.

The interladder interaction $V_{\text{out}2}$ are significantly smaller and thus will not bring any novel physics at higher energy scales (above 10 meV), so this leaves them out of the scope of this work.

VI. RENORMALIZATION GROUP STUDY

A. Statement of the problem with the interchain operators

The interactions with small momentum exchange can be absorbed in a definition of TLL parameters, but obviously there are also scattering channels with the large momentum exchange. These generate cosine-type terms, which, in principle, can bring us away from TLL universality class as defined in Eq. (3). There are several terms which are expressed as cosine operators in the bosonization language. In addition to previously incorporated umklapp terms there are the ones which emerge from the interchain interactions. It is because usually they are the most pertinent for the ladder system. They are

$q_1 = 2k_F$ these are interactions originating from the presence of $V_{\text{out}}(q = 2k_F)$, which have a form $\cos(2\phi_{\rho A})\cos(\sqrt{2}\phi_{\sigma 1})\cos(\sqrt{2}\phi_{\sigma 2})$;

$q_2 = 4k_F$ these are interactions originating from the presence of $V_{\text{out}}(q = 4k_F)$, which have a form $g_\perp^\pi \cos(4\phi_{\rho A})$, and (only in the commensurate case) the interchain umklapp $g_\perp^u \cos(4\phi_{\rho S})$;

$t_\perp$ the single-particle hopping induces several cosine operators,[39] each of them in the form $\cos(2\theta_{\rho A})F[\cos(\sqrt{2}\phi_{\sigma 1}), \cos(\sqrt{2}\phi_{\sigma 2})]$, where functional $F[]$ is a linear combination (there are also higher-order hopping terms, but as they are proportional to $t_\perp^2$ we can safely neglect them).

The standard way to treat these terms is deriving, perturbatively (usually on the single-loop level), the RG equations.[22] The RG equations allows us to predict whether a given term will increase and affect the low-energy physics (become

relevant) as the running energy variable $\Lambda \approx \max[\omega, T]$ decreases. To be precise, the quantity l entering to RG equations is defined as $\Lambda \sim \exp(-l)$ or to be precise $l = \ln(\Lambda/W)$, where $W = 2t$. This last formula makes it possible to link two quantities (which we do throughout this section); however, one should remember that while l is just a number, Λ has an energy unit. In the following we apply the following convention $g_\perp^\pi[\Lambda_1] = V_{\text{out}}(q = 4k_F)/\bar{\Lambda}$ where $\bar{\Lambda} = \pi v_F$.

The naive way would be to add RG equations describing these terms into the previously determined TLL fixed point. Unfortunately, in our particular problem this approach is not justified. Our problem can be stated as follows: How do we incorporate the above given operators into the intrachain, umklapp RG flow, which was already accounted for?

We expect that the following physics takes place. Around 200 meV a gapless TLL appears and later undergoes the renormalization flow. At this finite energy we know the values of interchain terms caused by $V_\perp(q = 4k_F)$ as they were estimated in the previous section, but g_3 cannot be taken to be equal to zero (it is not yet a fixed point, as explained in Sec. VI B). If we want to treat all instabilities with $4k_F$ periodicity on equal footing then we have to begin the flow with nonzero intrachain g_3 and see how it will compete or conspire with interchain instabilities. Estimating the value of the initial g_3 which we need to substitute into RG equations is a highly nontrivial task, our proposition on how to tackle this problem is given in Appendix C.

B. The intrachain, umklapp RG flow

In Sec. IV B we have given the values of intrachain TLL parameter K_ρ within the U-V model approximation. The point is that these are already renormalized, the fixed-point values K_ρ^*, and as such already contain influence of intrachain umklapp scattering.

The fact that this operator is there and affects K_ρ^* becomes clear from the following reasoning. As mentioned above, we are working with weakly dimerized chains close to half-filling. In the reduced Brillouin zone $k_F = 0.487\pi/b$ according to DFT[18] and $k_F = 0.51\pi/b$ according to ARPES.[40] This discrepancy can be understood. One should remember that the precise value of k_F can vary as it depends on the relative value of chemical potential inside a chain (determined also by strong correlations) with respect to the local potential on the Li ion (donor of electron). In any case one must admit that the doping is low enough, so in the high-energy regime the zig-zag chain is not able to recognize whether it is doped or not.

In addition, an important remark has to be kept in mind: The above form of umklapp operator is appropriate for a quarter-filled chain. This approach holds for a weakly dimerized zig-zag chain, to be precise, for the case when amplitude of the umklapp interaction is larger than dimerization. From the analysis of the DFT band structure we know that $t_1 - t_2 < 0.1$ eV. After evaluating the strength g_3 we also check if this assumption was consistent.

In this case the umklapp terms (so-called g_3), in the ith chain, in the form $\cos(\sqrt{8}\phi_{\rho i})$, have to be taken into consideration. The RG equation for this instability reads

$$\frac{\partial g_3}{\partial l} = 8g_3(1/4 - K_\rho). \qquad (16)$$

The critical value of TLL parameter for this operator is $K_\rho^c = 1/4$, so it seems to be irrelevant in our problem. However, in the case of Berezinskii-Kosterlitz-Thouless (BKT) flow, like the one described by Eq. (16) there exists a straight line on the $g_3 - K_\rho$ plane, a separatrix between relevance and irrelevance regime (gapped and critical phase). Essentially, this is because the compressibility of the charge mode will also change,

$$\frac{\partial K_\rho}{\partial l} = -8g_3^2 K_\rho^2 J_0(\delta^{\text{eff}}(l)), \qquad (17)$$

and for large-enough values of initial g_3, this equation cannot be neglected, the RG flow cannot be assumed to be vertical as we did before. Thus, the amplitude of bare coupling g_3 can play a role. As we see below, in our problem the amplitude g_3 does matter.

In Eq. (17) we kept the doping dependence which is encoded inside the Bessel function of the first kind $J_0(\delta(l))$. However, below we assume that doping is essentially equal to zero and we work in a commensurate case. This assumption comes from the fact that as we work in a constant chemical potential (the chain is embedded in a whole crystal and one knows the chemical potential of such a system from DFT solution) the effective doping will get renormalized $\sim -g_3^2 J_0(\delta^{\text{eff}}(l))$ already at higher energies. Because of the same reason we neglect the renormalization of the charge modes' velocity $\sim g_3^2 K_\rho J_2(\delta^{\text{eff}}(l))$. From now on all we neglect all doping dependence and set $\delta^{\text{eff}} = 0$ in the high-energy regime.

C. The RG analysis of the $4k_F$ terms

If the interchain $4k_F$ terms are considered alone then we immediately see that they are less relevant than the $2k_F$ instabilities described in Sec. VI D (it is because $K_{\rho\nu}^c = 1/2$). However, there are several reasons why we think that the $4k_F$ will be more important and decided to investigate it first. The $4k_F$ depends only on charge modes, which can be particularly important for energies larger than or comparable with J. What is more, as we deduced before, $K_\rho < 1/3$, and then it is the $4k_F$ CDW instabilities which are decaying slower. Finally, there is an intrachain umklapp term with the same periodicity and large, bare amplitude.

Section VI B gave us the necessary understanding of the intrachain RG flow; now we can proceed and introduce interchain terms. The $q_2 = 4k_F$ π-wave scattering has the RG equation

$$\frac{\partial g_\perp^\pi}{\partial l} = 2(1 - 2K_{\rho A})g_\perp^\pi - g_3 g_\perp^u \qquad (18)$$

and the interchain umklapp

$$\frac{\partial g_\perp^u}{\partial l} = 2(1 - 2K_{\rho S})g_\perp^u - g_3 g_\perp^\pi. \qquad (19)$$

In the above equations we have already introduced the so-called mixed terms caused by the presence of g_3 term (see below for an explanation). We need to take the interchain terms together with the standard umklapp g_3 to get a complete RG flow. These terms will also affect the flow TLL parameters, the $K_{\rho S,A}$, and the symmetric/asymmetric TLL parameters, which are defined in different basis than the intrachain $K_{\rho 1,2}$.

ones [used in Eqs. (16) and (17)]. The intrachain umklapp scattering may be rewritten in different basis than using the fact that the combination of two umklapps can be expressed in a rather simple form,

$$g_3[\cos(2\sqrt{8}\phi_{\rho 1}) + \cos(2\sqrt{8}\phi_{\rho 2})]$$
$$= 2g_3 \cos(4\phi_{\rho A}) \cdot \cos(4\phi_{\rho S}), \qquad (20)$$

where we assumed that umklapp g_3 is identical in both chains 1 and 2. This can be justified by the crystal symmetry argument.

In the following we work with the perturbation described by Eq. (20) in the symmetric/asymmetric basis. We need to rewrite the RG equations for the combined intrachain umklapp. Instead of Eqs. (16) and (17) now we have

$$\frac{\partial g_3}{\partial l} = g_3(2 - 4(K_{\rho S} + K_{\rho A})) + 2g_\perp^u g_\perp^\pi, \qquad (21)$$

$$\frac{\partial K_{\rho S}}{\partial l} = -K_{\rho S}^2 \left(8g_3^2 + (g_\perp^u)^2\right), \qquad (22)$$

$$\frac{\partial K_{\rho A}}{\partial l} = -K_{\rho A}^2 \left(8g_3^2 + (g_\perp^\pi)^2\right), \qquad (23)$$

where (in the last two equations) we have distinguished the two RG flows of symmetric and antisymmetric K_ρs [instead of single Eq. (17)] and already included their dependence on interchain interactions V_{out}. These equations should be taken together with Eqs. (18) and (19) to obtain the full RG flow. Below we show in Fig. 4 the result of a direct integration of this system of differential equations as well as a semiquantitative analysis of RG flow between energy scales corresponding to $\Lambda_1 = 0.2$ eV (where TLL is likely to form) and $\Lambda_2 = 0.02$ eV. These are the limits of interest for the high-energy regime study. The physical reason for this limit is given below.

One can dispute whether a direct integration is valid when g_3 and $y_\parallel$ (see Appendix C $y_\parallel$ definition) are of
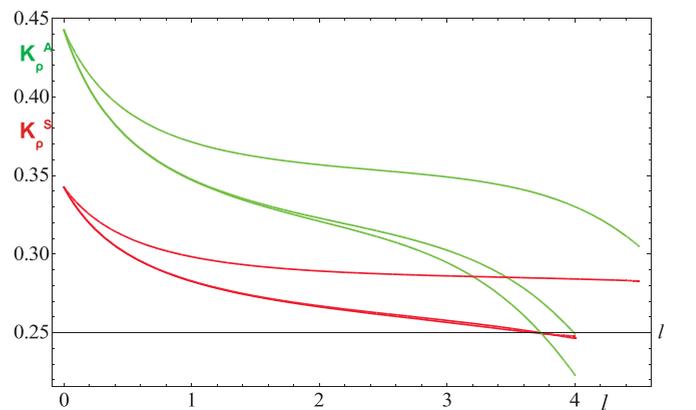

FIG. 4. (Color online) Three RG flows of $K_{\rho S}$ (red, three bottom curves at $l = 0$) and $K_{\rho A}$ (green, three top curves at $l = 0$) TLL parameters for different choices of initial parameters. The energy scale Λ_2 corresponds to $l \approx 3.5$. If all K_ν tend to be constant for increasing l, then the RG flow is called "vertical." The initial values for three curves are (from top to bottom) 0.03, 0.025, 0.35, 0.45, 0.35; 0.04, 0.035, 0.4, 0.45, 0.35; and 0.05, 0.04, 0.4, 0.45, 0.35, where the following notations are used: $g_\perp^\pi \bar\Lambda$, $g_\perp^u \bar\Lambda$, $g_3 \bar\Lambda$, $K_{\rho A}$, $K_{\rho S}$. For the RG flow which gives the bottom $K_{\rho S,A}$ curves, the instabilities (not shown) are large $g_i \approx 1/2$ at the scale $l \approx 5$ ($\Lambda_2 \Leftrightarrow l = 3.8$, which means that the RG flow should be stopped. The other flow does not suffer from this limitation.

order O(1). Such large terms could, in principle, generate significant higher-order operators along RG. However, there are no higher-order terms proportional to g_3^n ($n \geqslant 2$). Then the higher-order mixed terms will be either irrelevant [because of large p value in functional Eq. (5)] or of quite small amplitude. Qualitatively, the full RG flow can be thought as superposition of two BKT flows, two hyperbolas on the g_i-K_ν plane.

Let us first determine the amplitudes of different instabilities g_i at Λ_2 in the first-order approximation. If we neglect the flow of $K_\nu(l)$, then the solution of Eqs. (18), (19), and (21) is an exponential function:

$$g_\nu[2t * \exp(-l)] = g_\nu[\Lambda_1] \exp(\eta_\nu^*(-l - \ln(\Lambda_1/2t))), \quad (24)$$

where η_ν is the dimension of the operator g_ν, for example, $\eta_\perp^{\pi *} = 2(1 - 2K_{\rho A}^*)$. The crucial approximation we made in Eq. (24) is that we assumed exactly vertical flows and took the fixed-point values of K_ν^*, which tends to overestimate the strength of all instabilities. As a result of Eq. (24) we get $g_3[\Lambda_2]\bar{A} \approx 0.1$ eV, $g_\perp^\pi[\Lambda_2]\bar{A} \approx 0.075$ eV, and $g_\perp^u[\Lambda_2]\bar{A} \approx 0.08$ eV. Note that because initially $K_{\rho S}[\Lambda_1] < K_{\rho A}[\Lambda_1]$, the interchain umklapp $g_\perp^u$ renormalizes more than the π-DW one $g_\perp^\pi$; however, one has to remember that its bare amplitude is smaller due to doping effects. Already this simplified reasoning shows that the amplitude of the irrelevant term even at Λ_2 is still larger than amplitudes of the relevant terms. This is a peculiarity of our problem. The presence of a mixed term will, in fact, enhance this property: Because $g_\perp^u \approx g_\perp^\pi < g_3$ then one can interpret Eqs. (18) and (19) as if $K_{\rho S,A}^c$ was shifted from 1/2 downwards. On the other hand, in Eq. (21) we see that interchain instabilities push (weakly) the RG flow of g_3 towards its separatrix.

Now let us move to the analysis of the $K_{\rho S,A}$ RG flows. From Eqs. (22) and (23) we immediately realize that intra- and interchain terms support each other in lowering the values $K_{\rho S,A}$. Taking into account the initial (at Λ_1) hierarchy of energies we can be sure that the initial flow of $K_{\rho \nu} \sim g_i^2$ will be dominated by g_3^2 while the reasoning of the previous paragraph showed that around Λ_2 both terms are equally important. Initially the flow slows down because an irrelevant g_3 decreases, but later it can speed up again due to relevant interchain instabilities as seen on figure Fig. 4, where the result of numerically solving of Eqs. (22) and (23) is shown. Estimating quantitatively $K_{\rho S,A}[\Lambda_2]$ can be achieved in two ways.

The first way (i) assumes the independence of intra- and interchain BKT RG flows. We already know the influence of g_3 term alone; now we want to compute how much the $K_\nu[\Lambda_2]$ would be lowered during the BKT RG flow caused only by the interchain term, for example, if we keep only $g_\perp^\pi$ term in Eq. (23) for $K_{\rho A}[\Lambda_2]$. We can use the procedure very similar to the one applied in Appendix C, just that now we are moving towards $l \to \infty$ along the RG trajectory. By analogy with the Appendix C reasoning we define the flow invariant $A_\perp$. In the case of this RG flow $g_\perp^0 \approx 0.01 \ll 1$; thus, $A_\perp \approx (y^\perp)_\parallel^0$, where $(y^\perp)_\parallel^0 = 0.11$ is the distance of the bare $K_{\rho A}^0 = 0.39$ to $K_{\rho A}^c = 1/2$. We then obtain [from an analog of Eq. (C2)] that $y_\parallel^\perp[\Lambda_2] = 0.15$, which means that the RG flow caused $\Delta y_\parallel^\perp[\Lambda_2] = y_\parallel^\perp[\Lambda_2] - A_\perp \approx 0.05$ of the $K_{\rho A}[\Lambda_2]$ decrease.[41] This additional change of $K_{\rho A}[\Lambda_2]$ should be added on the
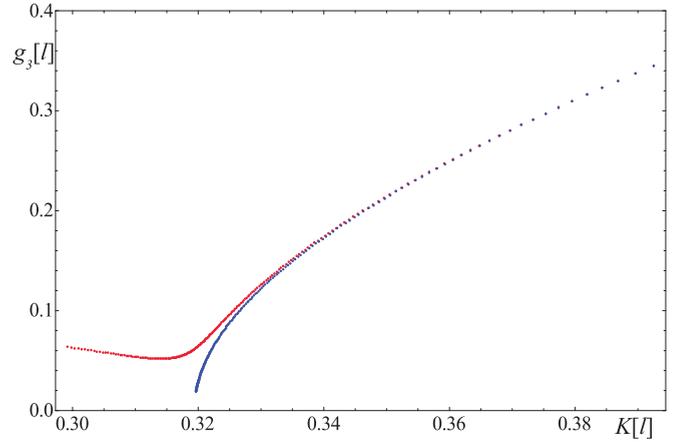

FIG. 5. (Color online) A comparison between BKT flow caused by a nonzero g_3 only (blue, bottom curve) and the result of our full RG flow (red, top curve). This is a parametric plot with $g_3[l]$ on the vertical axis and an average $K[l] = (K_{\rho S} + K_{\rho A})/2$ on the horizontal axis. The initial values are (for the blue line) 0.0, 0.0, 0.35, 0.45, and 0.35 and (for the red line) 0.03, 0.025, 0.35, 0.45, 0.35, with the same notation as in Fig. 4. The flow is shown down to $l = 5$.

top of the value previously found from the U-V model (see Sec. IV B) $K_{\rho A}^* \approx 1/3$. However, because of the g_3 influence, the $A_\perp$ is not a constant but it increases during the flow so the above value of the $\Delta y_\parallel^\perp[\Lambda_2]$ is underestimated. Such a deviation from a single BKT flow, particularly pertinent at lowest energies, is clear from figure Fig. 5.

The second way (ii) comes from the fact that, as pointed out above, the g_3 term dominates most of the RG flow between Λ_1 and Λ_2. Let us assume that the interchain terms effectively add up to the initial amplitude of $g_3[\Lambda_1]$ [see Eq. (20)],

$$g_3^{\text{eff}}[\Lambda_1] \approx g_3[\Lambda_1] + A_{\text{aux}} * 2 * V_{\text{out}}(4k_F)/\bar{A}, \quad (25)$$

where the origin of the $A_{\text{aux}} = 0.6$ factor is explained in the end of this section. Taking into account the results of Appendix C we see that with this new effective amplitude of the umklapp the initial point of the RG is located quite close to the separatrix of intrachain flow. The resulting value of $K_{\rho \nu}^*$ is then going to be close to $K_{\rho \nu}^c = 1/4$. This obviously overestimates the change of $K_{\rho \nu}[\Lambda_2]$ because effectively in Eq. (22) we took a square of a sum instead of a sum of squares. There is also a hidden assumption here that $K_{\rho A} \approx K_{\rho S}$, but looking at Fig. 4 we see that this works well for all cases.

From the reasonings (i) (upper limit) and (ii) (lower limit) we conclude that within our approximation $K_{\rho S,A} \in (0.25, 0.29)$. This is in agreement with the results presented in Figs. 4 and 5.

Finally, we can try to estimate the value of a gap in the holon spectrum. We choose to work with $g_\perp^\pi$ as it has the strongest tendency to open a gap. We estimate the gap in the case if this instability was acting on its own when $\Delta \approx W \exp(-l^*)$, where $g_\perp^\pi[W \exp(-l^*)] = 1$. For the specific cases the l^* is known,[22] for example, deep inside the gapped phase (self-consistent harmonic approximation) or close to the separatrix of RG. Unfortunately, our problem does not belong to any of these, because $A_\perp \approx 0.12$, which for Λ_2 energy scale is neither very small nor very large. We approximate the flow of the considered $g_\perp^\pi$ by BKT flow, which can be integrated out

(see also Appendix C):

$$\arctan\left(\frac{y_\parallel^0}{A_\perp}\right) - \arctan\left(\frac{y_\parallel}{A_\perp}\right) = A_\perp l. \tag{26}$$

If we use the fact that $y_\parallel^0 \approx A_\perp$ and $y_\parallel[2t\exp(-l^*)] \gg A_\perp$ (we are not far from the separatrix), then we get $A_\perp l^* \approx \pi/4$. In fact, this value of l^* is quite close to the ones we get from numerical integration of the full flow. Then the gap is

$$\Delta_\perp^\pi = 2t \exp[-\pi/(4A_\perp)], \tag{27}$$

which gives ≈ 2 meV. The low initial value of the $V_{\text{out}}(q = 4k_F)$ translates into quite small expected value of the gap in the spectrum.

The lowest energy (below Λ_2) flow of umklapp processes are seriously affected by doping. If the $g_\perp^\pi$ is able to open a gap before that, then these other RG equations will be changed by the presence of the gapped mode. For the intrachain umklapp instability the initial point lies very close (especially if we include terms beyond the U-V model) to the separatrix, which means that it is very susceptible to these modifications.

Usually in such a case one thinks about two competing instabilities taking place in two different basis (intra- and interchain). Our problem is different; the cooperation of instabilities is realized. This becomes clear if one assumes that the system tends to be locked at minimum, for example, corresponding to $\sqrt{8}\phi_{\rho1,2} = \pi$ [then $\cos(\sqrt{8}\phi_{\rho1,2}) = -1$]. For this specific value of $\phi_{\rho1,2}^0$ the combined interchain terms [see Eq. (20)] give nonzero and negative value ($A_{\text{aux}} \approx -0.6$). This corresponds to an additional energy gain caused by an auxiliary instability. It is a rare case when the two gaps do not exclude but can help each other. In particular this validates the assumption made in Eq. (25).

D. The analysis of the $2k_F$ terms

The RG equation for the $2k_F$ backscattering operator reads[22]

$$\frac{\partial g_\pi^{2k_F}}{\partial l} = (2 - K_{\rho A} - K_{\sigma A})g_\pi^{2k_F}. \tag{28}$$

It is the most relevant instability (already for $K_{\rho A} < 1$) if one assumes SU(2) symmetric case in the spin sector when $K_{\sigma A} = 1$, so naively we would expect it to dominate the low-energy physics. However, there are details that matter. First, the initial amplitude of this term is quite low. Second, the RG flow of this term will be strongly perturbed.

(i) At high energies ($\Lambda \approx 0.2$ eV) the spin sector is still in the incoherent regime; certainly the dispersion is not yet linear (mind the value of J_{eff}). Thus, all terms which contain spin dynamics, like $\cos(\phi_\sigma)$, will strongly fluctuate

(ii) The $2k_F$ terms have to compete with $4k_F$ instabilities described in the previous section: large g_3 (in the initial part of the flow) and relevant $g_\perp^\pi$ and $g_\perp^u$ in the lower energies

(iii) At lower energies (≈ 0.015 eV) several terms generated by the perpendicular hopping ($\sim t_\perp$) will start to intervene. Although they are irrelevant [connected with the field $\theta_{\rho A}$ (Ref. 39)], still their initial amplitude is significantly (three times) larger than $V_{\text{out}}(q = 2k_F)$. We then expect that physics will be dominated by a competition between these two types of cosine terms, as was studied in Refs. 42 and 43, where the term

confinement-deconfinement transition was coined to describe the physics.

Based on results from Refs. 42 and 43, one may expect that, due to last mechanism, the $2k_F$ instability is weakened. In any case, because $K_{\rho A} \ll K_{\rho A}^c = 1$ the $2k_F$-RG flow is vertical. This implies that the $K_{\rho A}$ value (and thus also Green's function α exponent) is very weakly affected by the presence of the $2k_F$ terms.

VII. DISCUSSION

A. Comparison with experiment

In this last part we wish to compare the estimated Luttinger liquid parameters with experimental findings. Experiments look at low-energy ($l > 1$), long-distance behavior ($r > k_F^{-1}$), which we should keep in mind for the rest of this section. The crucial question is as follows: What are the values of TLL parameters K_ν that enter into measured correlation functions? Obviously, the answer cannot depend on the point where we arbitrarily decide to stop the RG flow; one has to keep in mind that g_i terms usually are still finite at such a point. As discussed in Ref. 44, the correlation functions are of the form:

$$R(r) = \left(\frac{r}{W}\right)^{K^c} \exp\left(\int_0^{r/W} y_\parallel[l]dl\right), \tag{29}$$

where $|r| = \sqrt{x^2 + (v_\nu\tau)^2}$ is a distance in a time-space domain, W is an ultraviolet cutoff of the problem ($\sim 2t$), and $y_\parallel[l] = K_\rho - K_\rho^c$ is a deviation of TLL parameter from the critical value K_ρ^c of the considered flow. Thus, the observed value could be interpreted not as $K[l]$, but rather as weighted average of $K[l]$ over longer and longer length scales. In particular, if we flow to a gapless phase, then the observed K_ν corresponds to K_ν^*, which is then equal to the invariant of the flow A.

Our problem is particularly difficult, because the answer to the above question strongly depends on yet unknown lowest-energy physics. Indeed, in our reasoning we have neglected several effects [$t_\perp$, $D_{LS}(q = 2k_F)$, proximity to Mott insulator, disorder] whose amplitudes are certainly smaller than $\Lambda_2 \approx 20$ meV and which seriously harm TLL below this energy scale. Based on this we can reassure the validity of our approach only down to ~ 20 meV.

Basically, there are two distinct behaviors which can occur at these lowest-energy scales. First, one of the above-mentioned perturbations become pertinent just below the Λ_2 energy scale and thus stop the RG flow. In fact, all these perturbation in one way or another would not support further lowering of the K_ρ value; thus, the further $K_\rho[l]$ can be then taken as vertical. The observed TLL parameter should then be close to $K_\rho[\Lambda_2]$. The second possibility, which is not unlikely, is that 1D RG will remain valid down to much lower energies ~ 1 meV (see Sec. VII B). Then, as indicated in Fig. 5, the RG trajectory always stays close to the separatrix. This statement is, in fact, quantified by the values of invariants of the intra- and interchain RG flows: $A_3 \approx A_\perp$, so it is always either $g_3[l]$ or $g_\perp[l]$, keeping us close to the separatrix. Then Eq. (29) gives a power low with a $K_{\text{rho}}^c = 1/4$ exponent times a logarithmic corrections in the form $\log(r/W)$.

We are able to compare our results only with the experimental data corresponding to the high-energy range $\Lambda \in (0.02; 0.2)$ eV. In fact, this is also the energy scale down to which, with no experimental doubt, the TLL persists. One should also keep in mind that the TLL α exponent should be computed within the ladder model introduced in Sec. V B. In the following we assume that it is only K_ρ responsible for $\alpha \neq 0$, while $K_\sigma = 1$. Several different techniques have been used to measure the α exponent. These include PES[20] and ARPES[45,46] (4–150 meV; 5 K–300 K), STM[3](0–50 meV; 10 K–50 K), and resistivity[5,21](30 K–300 K), where in parentheses we have indicated temperature and frequency ranges where the fits were performed. We see that at least one of them is always larger than Λ_2, which makes our theory applicable. All probes are consistent and gave the spectral function exponent $\alpha \approx 0.55$–0.6, which means $\bar{K}_\rho \approx 0.24$–0.25. This is reasonably close to $K_{\rho S, A}[\Lambda_2] \in (0.25, 0.29)$ predicted theoretically in Sec. VI C, but also to $K_\rho^c = 1/4$. This shows the importance of the proximity to the Mott transition: It can cause a strong renormalization of K_ρ TLL parameters towards lower values and thus observe a large value of α exponent.

One can be even more explicit: The only way to obtain values $\alpha > 1/2$ (which translate into $K_\rho < 0.27$) in our model is by assuming that the combined $4k_F$ perturbations (intrachain g_3 together with $g_\perp^\pi$ and $g_\perp^u$ terms) can drive the RG flow and lead to strong renormalization of the charge TLL parameters. There is one more argument which supports this scenario. It is the lack of a spinon peak which has not been observed in any PES (or ARPES) experiment in the last two decades. This can be justified theoretically only if $\alpha > 1/2$, which provides strong limitations for the expected $\bar{K}_\rho^*$ values.

There is one experimental result which requires a comment. It is the temperature dependence of α invoked in Ref. 20, based on ARPES results. There the value $\alpha = 0.9$ was measured at high temperatures. This means $(K_{\rho S} + K_{\rho A})/2 + (K_{\rho S}^{-1} + K_{\rho A}^{-1})/2 \approx 6$, which translates to $\bar{K}_\rho^* \approx 0.17$. This value is much smaller than our predictions. We would like to emphasize that within TLL theory such behavior is very unlikely. To be precise, as explained above, it is not allowed to say that different points along the RG trajectory produce different observed values of K. One model can possibly have only one ground state described by $\bar{K}_\rho^*$. In our opinion the observed temperature dependence can originate from a significant influence which phonon occupancy has on the LDA band broadening.[17] The fact that $\alpha(T)$ dependence seems to change with sample preparation [see Fig. 3(d) in Ref. 20] strongly supports this interpretation. Then the real value of α is the low-energy one.

The other result is the estimate of a gap which, according to our reasoning, may be potentially opened by the $4k_F$ instabilities. However, the value has been found to be extremely small, ~ 1 meV; thus, our procedure, which relies on the RG analysis starting from 200 meV, is insufficient to make any definite claims. What is more, this value is much smaller than Λ_2, while there are several effects (like disorder or the interchain hopping $t_\perp$) which are potentially of order Λ_2 and destructive for such a gap. If the hierarchy of amplitudes was opposite (gap much larger than $t_\perp$), then the gap would suppress single-particle hopping. In our case the outcome is unclear. Certainly, a more sophisticated theory is necessary to

understand the unusual physics taking place below 20 meV. Experimentally, this is also a controversial issue. Such a gap [in the charge sector or in $A_{\text{TLL}}(\omega)$] has never been seen in any experiment probing $\omega > 3$ meV. So far the only exceptions are low temperature resistivity measurements,[5] but even there a clear Arhenius-type activation behavior (at around 1 meV) is preceded by an unusual power-law-like behavior.

B. The validity of 1D approximation

It is known[22] that the strong correlation effects (the formation of Luttinger liquid) are able to strongly reduce the value of $t_\perp$. To be more precise, they strongly reduce the energy scale where the system gains coherence along the c axis. With the value of the α exponent discussed above, the perpendicular hopping $t_\perp$ will get strongly renormalized down to an effective value,

$$t_\perp^{\text{eff}} = t \left(\frac{t_\perp}{t} \right)^{\left(\frac{1}{2-\zeta} \right)}, \tag{30}$$

where $\zeta = \alpha + 1$ is a single-particle Green's function exponent, and $\eta_{t\perp} = 2 - \zeta$ is a scaling dimension of the hopping operator. This gives a suppression of $t_\perp$ by a factor ≈ 20. To be precise, this means that, due to the presence of strong interactions, the hopping in the perpendicular direction becomes coherent only ≈ 1 meV.

On the top of it there is also another source of $t_\perp$ renormalization, which originates from the competition with the terms $V_{\text{out}}(q = 2k_F)$ (as described in Sec. VI D). The $2k_F$ terms, which are a functional of a charge asymmetric mode $\phi_{\rho A}$ (e.g., the one inducing a π-DW), tend to suppress $t_\perp$ (Ref. 43). Their influence is nonzero only when spin sector becomes coherent and $t_\perp$ is sufficiently small [there is a Bessel function $J_0(t_\perp[l])$ involved, which arises in a very similar way like the one in Eq. (17)]. It was shown[42,43] that the significant suppression of $t_\perp$ may happen only when $t_\perp[l] \approx V_{\text{out}}(q = 2k_F)$, which [according to scaling given in Eq. (30)] can be the case in our problem but only for energies below Λ_2.

The frustration of the nearest and the next-nearest perpendicular hopping also suppress the coherence of perpendicular hopping also on second order when, for example, particle-hole processes are considered. This is immediately visible if one writes a formula for any susceptibility $\chi(q, q_\perp, \omega)$ within the mean field, RPA level:

$$\chi(q, q_\perp, \omega)$$
$$= \frac{\chi^{\text{TLL}}(q, \omega)}{1 + (2t_\perp \cos(q_\perp c/2) + 2t'_\perp \cos(q_\perp c)) \chi^{\text{TLL}}(q, \omega)}, \tag{31}$$

where we are using a simplified version of perpendicular dispersion $\varepsilon(\vec{q_\perp})$ known from Eq. (A1). We see that the sign difference between $t_\perp$ and $t'_\perp$ can cause a suppression of a second term in the denominator. This obviously weakens the $q_\perp$ dependence of susceptibility (thus also a corresponding observable), but also has its influence if one wished to develop a perturbative series to study the influence of $t_\perp$.

Finally, there are also disorder effects which can localize carriers in the perpendicular direction. They are described in the next section.

From experiments (optical spectroscopy, Kadowaki-Woods ratio) we know that 1D physics seems to be correct even down to 2 meV. In light of the above discussion, these statements are not unreasonable. Thus, the assumption about the validity of 1D physics should be valid even down to few meV's and certainly in the high-energy range of energies (200–20 meV) on which this paper focuses. The values of TLL parameters indeed strongly support the idea that the 1D regime should be able to persist to temperatures much lower than the bare perpendicular hopping.

VIII. HOW PERTINENT IS SUBSTITUTIONAL DISORDER?

It seems that the most likely source of a disorder in purple bronze are random vacancies of Li atoms. From the DFT results[17] we know that energy shifts caused in this way within dispersive bands can be, at most, 15 meV (when the Li are completely removed). This sets the strength of the substitutional disorder potential. Because Li atoms are placed well outside zig-zag chains it is reasonable to assume the Coulomb potential interaction ($\sim q^2$) between impurity and TLL, with predominant small q-exchange scattering. Thus, the disorder will have primarily forward character and $D_f \approx 15$ meV.

Thus, we can assume the model of TLL with a forward disorder to check if it explains the observed temperature anomalies of ARPES below 200 K. The spectral function for forward disorder is known in real space,[22]

$$A(x,t) = A_{\text{TLL}}(x,t) \exp\left(-\frac{D_f K_\rho^2}{u_\rho^2}|x|\right), \quad (32)$$

where A_{TLL} is the pure Luttinger liquid spectral function, which is known [e.g., see Eq. (15)]. From this we immediately see that momentum integrated PES (response at $x = 0$) is the same as for a standard TLL. The additional broadening [second term in Eq. (32)] comes from random forward scattering with an assumption that scatterers are independently distributed in real space:

$$\langle W(x_i)W(x_j)\rangle = D_f \delta(x_i - x_j), \quad (33)$$

where $W(x)$ is a long-wavelength, real-space scattering potential at a given position x. The quantity which is observed in ARPES is a Fourier transform of Eq. (32), which is given by a convolution of TLL spectral function with the Lorentzian broadening:

$$A(q,\omega) = A_{\text{TLL}}(q,\omega) \otimes \left(\sqrt{\frac{2}{\pi}} \frac{D_f K_\rho^2/u_\rho^2}{\left[D_f K_\rho^2/u_\rho^2\right]^2 + q^2}\right). \quad (34)$$

The behavior of the Fourier transform is easy to extract in the certain limits, for example, of large and small ω. For the high-energy (15–150 meV) range we expect the A_{TLL} power law scaling (because we work above the energy range disorder can affect). This is definitely not seen in experimental data.[45] For the low energies (2–15 meV) we expect a convolution of standard TLL signal with an exponential decay. A broadening of A_{TLL} was indeed observed, however, already at 20 meV, which is larger than the maximal amplitude of disorder 15 meV. In addition, it was suggested[46] that the Gaussian

convoluted with the LL $A_{\text{TLL}}(q,\omega)$ provides better fit of the ARPES data. The assumption Eq. (33) was essential to get linear function of x in the exponent in Eq. (32). Thus, the Gaussian broadening suggested by experiment implies that the approximation of uncorrelated scattering events is not obeyed. The presumable presence of Gaussian broadening, in an analog of Eq. (34), suggests that the scattering events are not random, but momentum conserving.

Let us now move to a discussion of the random backward scattering. We expect that the forward (small q component) scattering D_f is accompanied with random scattering events with large momentum exchange D_b. By analogy with the reasoning done for $V_{\text{out}}(q)$ (see Sec. V A), which also has Coulomb-like character, we expect that $D_b \ll D_f$ [for a further estimation we take $D_b/D_f \approx V_{\text{out}}(q = 2k_F)/V_{\text{out}}(q = 0)$]. The amplitude of D_b should thus be <1 meV and thus should potentially affect only the lowest energy scales, lying beyond the scope of this paper. However, a brief discussion within TLL framework can be done. The D_b term has a cosine form, so it needs to be treated using the RG approach. We follow the same path as the one used for a single chain in Ref. 47:

$$\frac{\partial D_b}{\partial l}$$
$$= \left(3 - 1/2(K_{\rho A} + K_{\rho S}) - 1/2(K_{\sigma A} + K_{\sigma S}) - 2g_\pi^{2k_F}\right)D_b. \quad (35)$$

Taking into account that $K_\rho < 1$ and $K_\sigma \approx 1$ the D_b has to be highly relevant. However, the bare $D_b[\Lambda_0]$ is extremely small; thus, its dominance is questionable. The simplest way to answer this issue is by integrating the flow Eq. (35) with an extremely small initial $D_b[\Lambda_1]$, the previously estimated $K_v[l]$ (Sec. VI), and checking the value of disorder at energy scale Λ_2. This procedure suggests that localization length $\xi_{\text{loc}} \sim D_b^{-1}[\Lambda_2]$ would be rather long $\xi_{\text{loc}} \geqslant 30b$. This implies that the system is not prone to localization, in particular in the charge regime considered in this paper. However, the above-estimated ξ_{loc} is comparable with characteristic length caused by the doping δ away from quarter filling.

One can also notice that the D_b term competes with $2k_F$ instabilities which have larger bare amplitude and similar relevance than D_b. The RG equation for the $2k_F$ term also changes [compare with Eq. (28)],

$$\frac{\partial g_\pi^{2k_F}}{\partial l} = (2 - K_{\rho A} - K_{\sigma A})g_\pi^{2k_F} - \tilde{D}_b, \quad (36)$$

where $\tilde{D}_b = 2D_b\Lambda_0/\pi u_\rho^2$. The $2k_F$ terms do not have any simple, second-order contractions with the D_b term. There is also a change in the RG flow of the TLL parameters [e.g., in Eq. (17)], $\Delta\dot{K}_\rho \sim -K_\rho^2\tilde{D}_b$, induced by the presence of the backward disorder but we expect it to be negligibly small; thus, the RG flow is nearly vertical. In such a case the experimentally measurable α exponent should not be affected. The disorder breaks space-time invariance; thus, it induces renormalization (downwards) of holons velocity $\Delta\dot{u}_\rho \sim -K_\rho\tilde{D}_b$, which is similar to the umklapp-induced velocity renormalization.

If one assumes the validity of the 1D TLL regime below the Λ_2 energy scale, then certain comparisons with experiments

are possible. These experimental findings suggest that the backward disorder does not dominate the low-temperature physics. It is known that in 1D systems the backward disorder, when present, kills the superconductivity.[22] This has been indeed observed for more disordered samples of purple bronze where the superconductivity disappears.[21] However, the physics at higher energies $\sim \Lambda_2$ was unaffected by the D_b. The unusually broad ARPES lines (the strongest indication of a new physics at energies around 100 K) were clearly observed for all samples including the superconducting ones.[46] The pertinence of disorder also does not fit well with either magnetoresistivity[5] or STM[3] experiments. The power laws implied by weak localization do not fit with resistivity temperature dependence between 20 K and 300 K.[21,48] It is also claimed (from optical spectroscopy[7]) that the mass of remaining mobile carriers decreases below 30 K.

In conclusion, this simplest notion of disorder in TLL is incompatible with observed effects. However, the discussion is not yet closed. The crystal structure is quite complex and supports much more sophisticated mechanisms, for example, the relative rotations of different Mo octahedra which may strongly affect the hopping (overlap integrals) between Mo sites. Such rotations could provide another source of disorder in the material; this time the $t_i's$ parameters will be affected. Some of these effects were studied (via atoms shifting) in Ref. [17], and it was found that the amplitude of such effects is similar to D_f. What is certain is that all these microscopic effects should affect $t_\perp$ more strongly than the inside-chain TLL physics, because $t_\perp \approx D_f$ (while t is two orders of magnitude larger). This means that the relative strength of disorder is quite large when the perpendicular coherence is considered. One has to remember that, although discussing standard disorder within the TLL framework is a straightforward extensions of previous works,[47] the other mechanisms requires a separate study, clearly beyond the scope of the present paper.

IX. CONCLUSION

We studied the low-energy physics of a quasi-1D material, lithium molybdenum purple bronze. Already before it has been shown that this material is extremely anisotropic, there is a linear dispersion along the b axis extending down to 0.4 eV, while in the perpendicular direction dispersion is at least two orders of magnitude weaker. In this study the physics is expressed in terms of field theory. Our work covers the energy range where the physics of charge modes, holons, describes well the dynamics of the compound. It begins at around 0.2 eV, where the experiment has clearly shown an emergence of 1D spectral properties, in particular the fermionic bands seem to merge at this energy scale giving rise to a single entity. The regime of our interest extends as low as 1D physics is strictly valid. To be on the safe side we set it at around 20 meV, which is larger than any of the possible disturbances.

The starting point of our study is the recent LDA-DFT result where the peculiar band structure of the material has been reconfirmed. Based on this we construct the effective low-energy theory: The band structure around Fermi energy is cast into a tight-binding model. In addition, a minimal model has to contain the strong correlation terms, laying beyond LDA-DFT

approximation. The aim of the next few sections is to provide the quantitative description of these strong interactions.

We begin with parametrizing the interactions inside a single zig-zag chain. From previous experimental and numerical works we are able to extract an effective real-space model with a physically reasonable values of strong correlation parameters. Due to sparse arrangement of the chains, the interactions have a finite range character; however, in the first approximation we use the U-V model to obtain the values of Luttinger liquid parameter K_ρ. This estimate is based on several numerical works dedicated for models which are very similar to ours. All values converge at $K_\rho \approx 1/3$, which is a rather low value; in particular, it may allow $4k_F$ instabilities to dominate the physics. It also suggests that the umklapp processes are at play. In addition we also investigate the effects which can arise if one goes beyond the simplistic U-V model. A separate section is dedicated to the spin sector, where we estimate basic energy scales.

Later parts of this work are devoted to interchain physics. As the chains are grouped in well-distinguishable pairs, it is tempting to propose a description within a ladderlike model. We use dielectric approximation in order to estimate strength of interchain interactions, considering processes with both small and large momenta exchange. With this knowledge we propose that the description of physics in the considered charge regime should be done within the framework of Luttinger liquid consisting of four modes, the two charge modes corresponding to the total (symmetric) and the transverse (asymmetric) fluctuations. This description fully incorporates the interchain processes with small momentum exchange together with the intrachain physics.

The interchain processes with large momentum exchange can be taken as perturbation and treated within the RG approach. However, we claim that in order to achieve a valid description of the system one has to consider the intrachain umklapp together with them. We derive a full system of RG equations which cover intra- as well as interchain instabilities and study possible trajectory of the flow. This allows us to develop a description of purple bronze down to the limits of validity of 1D theory. In the discussion we show that these limits can be safely extended to energy scales two or even three times smaller than 20 meV. This allowed us to make a more extensive, quantitative comparison with experimental results, which basically confirms our theoretical insight into this complicated compound.

We have achieved the effective low-energy description of $Li_{0.9}Mo_6O_{17}$ compound, which is able to explain convincingly experimental findings down to 20 meV. In particular, we showed that for the specific combination of parameters, which are present in this material, an unusual situation may occur. Due to their mutual competition, the critical phase (the Luttinger liquid) is able to survive down to the very low energy scales. Despite the two leg ladder formation, no gap opens in the holon spectra (at least not above 20 meV). This is contrary to the usual case where a significant gap is present in a transverse (asymmetric) mode of a ladderlike low-dimensional system. Such an unusual physics is in agreement with the physics extracted from experimental investigations.

It is likely that for the lowest energies the purple bronze falls into the category of doped Mott insulators with extremely small

gap, but further developments of the theory are necessary to make any definite claims about this highly interesting regime.

Note added. Recently, we became aware of a study by Merino *et al.*,[49] which uses a different methodology to obtain similar values for the effective parameters as the ones we obtain in Table II.

APPENDIX A: DERIVATION OF TIGHT-BINDING PARAMETERS

The central result of DFT calculation is a band structure of a given material. As it contains a huge amount of information, usually it is difficult to deal with when the effective, low-energy theory is constructed. In such a case a standard procedure is to approximate a solid by a tight-binding model with a selected sites located at their positions r_i and unknown hopping parameters between them. Usually only the nearest t and the next-nearest t' neighbor hoppings are taken into account. We are interested in the low-energy physics; thus, the aim is to fit bands crossing Fermi energy E_F (in the given direction d) with the properly chosen parameters t_d t'_d.

As described in Sec. II in the case of $Li_{0.9}Mo_6O_{17}$ most of the low-energy spectral weight is located on Mo(1) and Mo(4) sites [see Fig. 1(a)] so we take only them into further considerations. As explained, only two bands cross E_F; thus, our aim is to fit these two dispersions.

The dispersion relation for tight-binding model defined above is known:

$$
\begin{aligned}
\varepsilon(\vec{k}) = & -t\cos(k_b b/2) - t'\cos(k_b b) \\
& - \frac{t_{\perp 1} + t_{\perp 2}}{2}\cos(k_c c/2) - \frac{t_{\perp 1} - t_{\perp 2}}{2}\sin(k_c c/2) \\
& - \frac{t'_{\perp 1} + t'_{\perp 2}}{2}\cos(k_c c) - \frac{t'_{\perp 1} - t'_{\perp 2}}{2}\sin(k_c c), \quad \text{(A1)}
\end{aligned}
$$

where the first line describes the dispersion along the b axis and the last two lines describe the dispersion along the c axis (with the dimerization included). We neglected dispersion along the a axis. For the b-axis dispersion we assumed the simplest tight-binding model, as the LDA result suggests a rather straightforward interpretation of the bands. We introduced next-nearest-neighbor hopping t' mostly because the zig-zag chain structure seems to allow for this refinement; however, from the general shape of bands in the $\vec{b}$ direction, it does not seem to be necessary.

For the c-axis dispersion the situation is quite different. We introduced many more terms because the curve is quite unusual, with a well-pronounced double minima and a node at $k_c = 0$, a feature quite difficult to fit within standard model. Based on the analysis of the structure presented in Fig. 1(a) we deduce that

  (i) there are two times more intraladder than interladder links [they are linked either directly through Mo(1)-Mo(4) bond or auxiliaries through Mo(2)-Mo(5) bond];
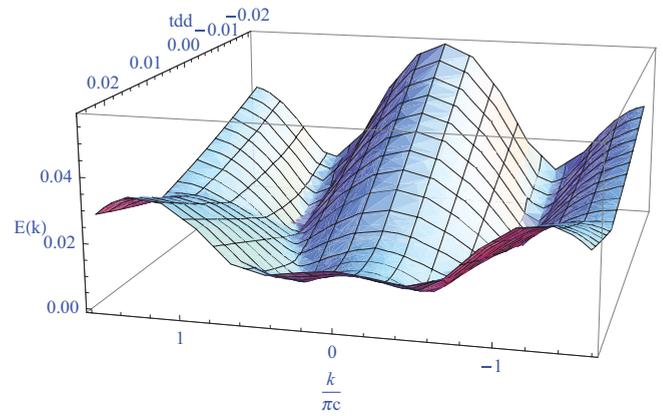

FIG. 6. (Color online) The dispersion along c axis shown for varying direct δ hopping $t_{dd} \equiv t_{\perp 1}$ along Mo(1)-Mo(4) bond. The strength of the other hopping path [through Mo(2)-Mo(5)] $t'_{\perp 1}$ is taken as -0.02 while the interladder one $t'_{\perp 2}$ is -0.01.

  (ii) the interladder hopping goes always though Mo(2) [or Mo(5)] atoms, these are two paths which can interfere (these hoppings are possible only every second site);

  (iii) the next-nearest-neighbor hopping is allowed only through Mo(2)-Mo(5) and thus should be much smaller than the one above (these hoppings are also possible only every second site).

All of the hoppings go either via a δ bonds or π bonds (the second are allowed only due to octahedra tilting). None of the links should be very much stronger than the others. From the crystal structure analysis all other hoppings should be negligible; thus, the task is to fit the dispersion with the above given model Eq. (A1).

In Fig. 6 we show an example of k_c dispersion with conditions (i)–(iii) fulfilled. We see that it is possible to obtain a shape quite similar to the LDA one provided that two interfering paths have the hopping parameters of the opposite sign. The only quantitative issue would be a relatively large value of band splitting found in Ref. 17. It may appear from the Hartree interaction term if the two bands had different orbital character. One should also remember that the value of splitting found in Ref. 18 was a bit smaller. We will leave this issue for further specialized studies like, for example, Nth-order Muffin-Tin Orbital (NMTO) method.

These findings are summarized in Table I. Similar values were found in Ref. 49.

APPENDIX B: DERIVATIONS OF THE COSINE TERMS

We begin with a fermionic for the considered scattering processes: (1) the intrachain umklapp,

$$
\begin{aligned}
H^i_{\cos 3} = g_3 \sum_{q_i} (& \psi^\dagger_{+q_1 i\uparrow}\psi^\dagger_{+q_2 i\downarrow}\psi_{-q_3 i\downarrow}\psi_{-q_4 i\uparrow} \\
& + \psi^\dagger_{-q_1 i\uparrow}\psi^\dagger_{-q_2 i\downarrow}\psi_{+q_3 i\downarrow}\psi_{+q_4 i\uparrow}); \quad \text{(B1)}
\end{aligned}
$$

(2) interchain umklapp scattering ($4k_F$),

$$
\begin{aligned}
H^\perp_{\cos 3} = g^\perp_3 \sum_{q_i} (& \psi^\dagger_{+q_1 1\uparrow}\psi^\dagger_{+q_2 2\downarrow}\psi_{-q_3 2\downarrow}\psi_{-q_4 1\uparrow} \\
& + \psi^\dagger_{-q_1 1\uparrow}\psi^\dagger_{-q_2 2\downarrow}\psi_{+q_3 2\downarrow}\psi_{+q_4 1\uparrow}), \quad \text{(B2)}
\end{aligned}
$$

where the following relation between momenta holds $q_1 + q_1 - q_1 - q_1 = 0$ in order to preserve momentum conservation during scattering (the low-energy limit implies that for each momenta there exist the ultraviolet cutoff $|q_i| < \Lambda$);

(3) interchain exchange scattering ($4k_F$),

$$H_{\cos}^{\pi} = g_{\pi}^{4k_F} \int_0^L dx \rho_1^{4k_F} \rho_2^{4k_F}; \qquad (B3)$$

(4) interchain exchange scattering ($2k_F$),

$$H_{\cos}^{\pi} = g_{\pi}^{2k_F} \int_0^L dx \rho_1^{2k_F} \rho_2^{2k_F}, \qquad (B4)$$

where $\rho_i^{2k_F}$ is the $2k_F$ charge density in the ith chain.

Usually one is also interested in correlation functions, which have the general form

$$R_O = \langle T_\tau O(x,t) O^\dagger(0,0) \rangle, \qquad (B5)$$

where the simplest intrachain examples of possible operators O are

(i) in Peierls channel, the charge density wave (CDW),

$$O_{\mathrm{CDW}}(x,t) = \sum_{r,\sigma,\sigma'} \psi_r(x,t)^\dagger \delta_{\sigma\sigma'} \psi \bar{r}(x,t);$$

(ii) in Cooper channel, the singles superconductivity (SS),

$$O_{SS}(x,t) = \sum_{r,\sigma,\sigma'} \sigma \psi_r(x,t) \delta_{\sigma\bar{\sigma}'} \psi_{\bar{r}}(x,t).$$

When we consider a single chain, then a chiral fermion creation operator is related to bosonic spin and charge fields as follows (in the continuum limit):

$$\psi_{r,\sigma}(x) = \frac{1}{\sqrt{2\pi\alpha}} \eta_{r,\sigma} \exp(\iota r k_F x) \exp{-\iota/\sqrt{2}(r\phi_\rho(x) - \theta_\rho(x)} \\ + \sigma(r\phi_\sigma(x) - \theta_\sigma(x))), \qquad (B6)$$

where the coefficient $\eta_{r,\sigma}$ is the Majorana fermion which does not have any spatial dependance and it is introduced only in order to preserve anticommutation for the fermion operators ψ. Usually they do not play any role in the physical description of the system but they are able to change signs of some correlation functions, so one has to take care about them.

In the case of the ladder one has a straightforward generalization:

$$\psi_{r,\sigma,\nu}(x,t) \sim \eta_{\sigma,\nu} \exp(\iota r k_F x) \exp\left[-\frac{\iota}{2}(r\phi_{+\rho} + \theta_{+\rho} \\ + \sigma(r\phi_{+\sigma} + \theta_{+\sigma}) + \nu(r\phi_{-\rho} + \theta_{-\rho} \\ + \sigma(r\phi_{-\sigma} + \theta_{-\sigma})))\right]. \qquad (B7)$$

The above-given equations [Eqs. (B6) and (B7)] make it possible to rewrite all fermionic terms in the Hamiltonian like, for example, the one in Eq. (B1) or, in general, any interesting operator in the language of bosonic fields. In our particular case we are interested in the following interaction terms:

(1) umklapp scattering (at quarter filling) in the ith chain,

$$H_{\cos3} = g_3 \int_0^L dx \cos(2\sqrt{8}\phi_{i\rho}(x) + \delta), \qquad (B8)$$

where δ indicates the doping away from a commensurate case, quarter filling in our case [where $\exp \iota(\pi - 4k_F)x$ is not oscillating];

(2) interchain umklapp scattering ($4k_F$),

$$H_{\cos3}^{\perp} = g_3^{\perp} \int_0^L dx \cos(4\phi_{S\rho}(x) + \delta); \qquad (B9)$$

(3) interchain exchange scattering ($4k_F$),

$$H_{\cos}^{\pi} = g_{\pi}^{4k_F} \int_0^L dx \cos(4\phi_{A\rho}(x)); \qquad (B10)$$

(4) interchain exchange scattering ($2k_F$),

$$H_{\cos}^{\pi} = g_{\pi}^{2k_F} \int_0^L dx \cos(2\phi_{A\rho}(x)) \cos(\sqrt{2}\phi_{1\sigma}(x)) \\ \times \cos(\sqrt{2}\phi_{2\sigma}(x)). \qquad (B11)$$

These are the terms for which RG equations are derived in Sec. VI. In all the above we took the convention

$$\phi_{S,A}(x) = \frac{\phi_1(x) \pm \phi_2(x)}{\sqrt{2}}, \qquad (B12)$$

which makes it possible to go from one basis to another.

APPENDIX C: INITIAL VALUES OF UMKLAPP TERMS

Estimating the value of g_3 at certain energy scale Λ_0 is an impossible task, so all of our results cannot be taken strictly quantitatively. This is a generic problem of the RG method present for any model even a simple half-filled chain. The complexity of our system makes the task even more tedious.

We propose the approach, based on the first-order expansion of RG equations, to get a reasonable value of $g_3(\Lambda_0)$. However, one has to keep in mind that because we are are working with rather large couplings, of order 0.1 (but always smaller than 0.25), higher-order terms can introduce non-negligible corrections even within single instability flow. Thus, the results have to be taken with caution and can be thought of as only approximation.

With these remarks being said we can proceed. One can, in principle, integrate out BKT equations to get values for along the flow. One gets the following result:[22]

$$g[l] = \frac{A}{\sinh[Al + \tanh^{-1}(A/y_\parallel^0)]}, \qquad (C1)$$

$$y_\parallel[l] = \frac{A}{\tanh[Al + \tanh^{-1}(A/y_\parallel^0)]}, \qquad (C2)$$

where A is an invariant of the flow, in our case $A = 1/12$. Every point on an RG trajectory leads us to fixed point value K_{rho}^*. From numerics based on U-V model we found (Sec. IV B) $K_{\mathrm{rho}}^* = 1/3$ and we know that for quarter-filled chain $K_{\mathrm{rho}}^c = 1/4$. Thus, in our case $A = K_{\mathrm{rho}}^* - K_{\mathrm{rho}}^c = 1/12$. Our aim is to extract the value of $K_{\mathrm{rho}}[l] = K_{\mathrm{rho}}^c + y_\parallel[l]$ at a certain energy scale Λ_1 (corresponding to ≈ 0.2 eV), which upon RG leads to known K_{rho}^*. This procedure can be thought as moving against the direction of the RG flow.

The only missing quantity in Eq. (C1) is $y_\parallel[l = 0]$, which should be interpreted as the distance of an initial point of the flow $K_{\mathrm{rho}}[l = 0]$ (formally in the infinite energy, i.e.,

somewhere around UV-cutoff of the model) from $K_{rho}^c = 1/4$. Although around the fixed point the flow is rather vertical, we decided to take the most conservative [and giving the most modest value of $g_3(\Lambda_0)$] assumption that $K_{rho}[l = 0] = 1/2 \Rightarrow y_{\parallel}[l = 0] = 1/4$. It is because certainly at $K_{rho} = 1/2$ the quarter-filled chain remains insensitive to Mott localization.

With this we are able to estimate the bare $g_3[\Lambda_1]\bar{\Lambda}$ to be around 0.4 eV. The position of the separatrix of RG flow in the first order is set by $y_{\parallel} = g$ and from our considerations we see that the difference $y_{\parallel}[\Lambda_1] - g[\Lambda_1]$ is an order of magnitude smaller than $y_{\parallel}[\Lambda_1]$. The distance from the separatrix is of the same order as additional intrachain terms described in Sec. IV C. From the remarks above we know this is only an estimate, but it certainly implies that the umklapp, even in intrachain U-V approximation, is an order of magnitude larger than any of the $V_{\perp}(q = 4k_F)$. Although it seems to be irrelevant, its bare amplitude is large and quite close to the separatrix so the intrachain umklapp has to be taken with care in the RG analysis below.

The fact that bare g_3^0 falls very close to the separatrix can be confirmed by an independent reasoning. The position of the separatrix is frequently constrained by symmetry considerations. Taking into account the hierarchy of energy scales, we take simplistic approximation of spinless fermions in $U \to \infty$ (like in Sec. IV B). This obviously overestimates g_3, but numerics[29] show us that beyond a threshold $U = 4t$, the dependence on U is weak; thus, the corrections breaking (particle-hole) symmetry should be quite small. The advantage is that now one can map the charge sector on the pseudospin model (empty and occupied sites), for which the position of the separatrix of RG flow (phase transition) in terms of bare parameters is known exactly thanks to SU(2) symmetry. It is located at $V_{in}^{eff^c} = 2t^{eff}$, where V_{in}^{eff} accounts for all unscreened interactions along the chain (while $t^{eff} \approx t$, if one wants to be more precise, one would find it slightly reduced with respect to t because of dimerization). If we use values found before (in Table III for V_{in}^{eff}) we indeed find ourself very close to $V_{in}^{eff^c}$.

---

[1] W. H. McCarroll and M. Greenblatt, J. Solid State Chem. **54**, 282 (1984).

[2] J. D. Denlinger, G.-H. Gweon, J. W. Allen, C. G. Olson, J. Marcus, C. Schlenker, and L.-S. Hsu, Phys. Rev. Lett. **82**, 2540 (1999).

[3] J. Hager, R. Matzdorf, J. He, R. Jin, D. Mandrus, M. A. Cazalilla, and E. W. Plummer, Phys. Rev. Lett. **95**, 186402 (2005).

[4] M. Greenblatt, W. H. McCarroll, R. Neifeld, M. Croft, and J. V. Waszczak, Solid State Commun. **51**, 671 (1984).

[5] Xiaofeng Xu, A. F. Bangura, J. G. Analytis, J. D. Fletcher, M. M. J. French, N. Shannon, N. E. Hussey, J. He, S. Zhang, D. Mandrus, and R. Jin, Phys. Rev. Lett. **102**, 206602 (2009).

[6] Nicholas Wakeham, Alimamy F. Bangura, Xiaofeng Xu, Jean-Francois Mercure, Martha Greenblatt, and Nigel E. Hussey, Nat. Commun. **2**, 396 (2011).

[7] J. Choi, J. L. Musfeldt, J. He, R. Jin, J. R. Thompson, D. Mandrus, X. N. Lin, V. A. Bondarenko, and J. W. Brill, Phys. Rev. B **69**, 085120 (2004).

[8] J. L. Cohn, B. D. White, C. A. M. dos Santos, and J. J. Neumeier, Phys. Rev. Lett. **108**, 056604 (2012).

[9] J. Chakhalian, Z. Salman, J. Brewer, A. Froese, J. He, D. Mandrus, and R. Jin, Physica B **359**, 1333 (2005).

[10] M. Onoda, K. Toriumi, Y. Matsuda, and M. Sato, J. Solid State Chem. **66**, 163 (1987).

[11] C. A. M. dos Santos, B. D. White, Yi-Kuo Yu, J. J. Neumeier, and J. A. Souza, Phys. Rev. Lett. **98**, 266405 (2007).

[12] M. S. da Luz, J. J. Neumeier, C. A. M. dos Santos, B. D. White, H. J. Izario Filho, J. B. Leão, and Q. Huang, Phys. Rev. B **84**, 014108 (2011).

[13] G.-H. Gweon, J. W. Allen, and J. D. Denlinger, Phys. Rev. B **68**, 195117 (2003).

[14] G.-H. Gweon, J. D. Denlinger, J. W. Allen, C. G. Olson, H. Höchst, J. Marcus, and C. Schlenker, Phys. Rev. Lett. **85**, 3985 (2000).

[15] Feng Wang, S.-K. Mo, J. W. Allen, H.-D. Kim, J. He, R. Jin, D. Mandrus, A. Sekiyama, M. Tsunekawa, and S. Suga, Phys. Rev. B **74**, 113107 (2006).

[16] G.-H. Gweon, S.-K. Mo, J. W. Allen, J. He, R. Jin, D. Mandrus, and H. Höchst, Phys. Rev. B **70**, 153103 (2004).

[17] Thomas Jarlborg, Piotr Chudzinski, and Thierry Giamarchi, Phys. Rev. B **85**, 235108 (2012).

[18] Z. S. Popović and S. Satpathy, Phys. Rev. B **74**, 045117 (2006).

[19] Myung Hwan Whangbo and Enric Canadell, J. Am. Chem. Soc. **110**, 358 (1988).

[20] Feng Wang, J. V. Alvarez, S.-K. Mo, J. W. Allen, G.-H. Gweon, J. He, R. Jin, D. Mandrus, and H. Höchst, Phys. Rev. Lett. **96**, 196403 (2006).

[21] C. A. M. dos Santos, M. S. da Luz, Yi-Kuo Yu, J. J. Neumeier, J. Moreno, and B. D. White, Phys. Rev. B **77**, 193106 (2008).

[22] T. Giamarchi, *Quantum Physics in One Dimension* (Oxford University Press, Oxford, 2004).

[23] Ersoy Şaşıoğlu, Christoph Friedrich, and Stefan Blügel, Phys. Rev. B **83**, 121101 (2011).

[24] C. S. Jacobsen, J. Phys. C **19**, 5643 (1986).

[25] Frédéric Mila, Phys. Rev. B **52**, 4788 (1995).

[26] Alejandro M. Lobos and Thierry Giamarchi, Phys. Rev. B **82**, 104517 (2010).

[27] F. D. M. Haldane, Phys. Rev. Lett. **47**, 1840 (1981).

[28] S. Ejima, F. Gebhard, and S. Nishimoto, Europhys. Lett. **70**, 492 (2005).

[29] F. Mila and X. Zotos, Europhys. Lett. **24**, 133 (1993).

[30] Satoshi Ejima, Florian Gebhard, and Satoshi Nishimoto, Phys. Rev. B **74**, 245110 (2006).

[31] K. Sano and Y. Ōno, Phys. Rev. B **70**, 155102 (2004).

[32] Martin Hohenadler, Stefan Wessel, Maria Daghofer, and Fakher F. Assaad, Phys. Rev. B **85**, 195115 (2012).

[33] Gregory A. Fiete, Rev. Mod. Phys. **79**, 801 (2007).

[34] R. J. Iverson and L. Hodges, Phys. Rev. B **8**, 1429 (1973).

[35] In a thin layer of a semiconductor MoO_3 (a material with locally similar structure) the measured value is $\kappa = 2.5$.[36]

[36] Krishnaji Parmendu Kant and Ramji Srivastava, J. Phys. Soc. Jpn. **39**, 1316 (1975).

[37] H. Schulz, in Proceedings of Les Houches Summer School, LXI, edited by E. Akkermans, G. Montambaux, J. Pichard, and J. Zinn-Justin (Elsevier, Amsterdam, 1995), p. 533.

[38] Dror Orgad, Philos. Mag. B **81**, 377 (2001).

[39] D. V. Khveshchenko and T. M. Rice, Phys. Rev. B **50**, 252 (1994).

[40] G.-H Gweon, J. D. Denlinger, J. W. Allen, R. Claessen, C. G. Olson, H. Höchst, J. Marcus, C. Schlenker, and L. F. Schneemeyer, J. Electron Spectrosc. Relat. Phenom. **117-118**, 481 (2001).

[41] Because $A_\perp \approx y_\perp^0$, one needs to take Taylor expansion of tanh function in Eq. (C1).

[42] M. Tsuchiizu, P. Donohue, Y. Suzumura, and T. Giamarchi, Eur. Phys. J. B **19**, 185 (2001).

[43] M. Tsuchiizu and Y. Suzumura, Phys. Rev. B **59**, 12326 (1999).

[44] T. Giamarchi and H. J. Schulz, Phys. Rev. B **39**, 4620 (1989).

[45] Feng Wang, J. V. Alvarez, J. W. Allen, S.-K. Mo, J. He, R. Jin, D. Mandrus, and H. Höchst, Phys. Rev. Lett. **103**, 136401 (2009).

[46] J. W. Allen, Lenart Dudy, Feng Wang, J. He, A. Sekiyama, and S. Suga, arXiv:1206.0798.

[47] T. Giamarchi and H. J. Schulz, Phys. Rev. B **37**, 325 (1988).

[48] J.-F. Mercure, A. F. Bangura, Xiaofeng Xu, N. Wakeham, A. Carrington, P. Walmsley, M. Greenblatt, and N. E. Hussey, Phys. Rev. Lett. **108**, 187003 (2012).

[49] Jaime Merino and Ross H. McKenzie, Phys. Rev. B **85**, 235128 (2012).